

Water Resources Research

RESEARCH ARTICLE

10.1029/2019WR026284

Key Points:

- Developed an Integrated Drought Index based on meteorological, hydrological, and agricultural droughts
- IDI uses SPI, SRI, SSI, and SGI by incorporating the response of precipitation, runoff, soil moisture, and groundwater
- IDI performs well against the Drought Severity Index (DSI) and groundwater well and streamflow observations

Supporting Information:

- Supporting Information S1

Correspondence to:

V. Mishra,
vmishra@iitgn.ac.in

Citation:

Shah, D., & Mishra, V. (2020). Integrated Drought Index (IDI) for drought monitoring and assessment in India. *Water Resources Research*, 56, e2019WR026284. <https://doi.org/10.1029/2019WR026284>

Received 4 SEP 2019

Accepted 16 DEC 2019

Accepted article online 18 DEC 2019

Integrated Drought Index (IDI) for Drought Monitoring and Assessment in India

Deep Shah¹  and Vimal Mishra¹ 

¹Department of Civil Engineering, Indian Institute of Technology (IIT), Gandhinagar, India

Abstract Drought monitoring and declaration in India are challenging due to the requirement of multiple drought indices representing meteorological, hydrological, and agricultural droughts that are often not available in near real-time. In addition, the current drought monitoring efforts do not consider groundwater storage variability. To overcome this, we develop an Integrated Drought Index (IDI) that combines the response of meteorological, hydrological, and agricultural droughts and accounts for groundwater storage. We use the Gaussian copula to integrate the 12-month Standardized Precipitation Index (SPI), 4-month Standardized Runoff Index (SRI), 1-month Standardized Soil moisture Index (SSI), and 1-month Standardized Groundwater Index (SGI) to develop IDI. Hydrologic variables (total runoff, soil moisture, and groundwater) required in IDI were simulated using the Variable Infiltration Capacity (VIC) with SIMple Groundwater Model (VIC-SIMGM). We evaluated IDI against the Drought Severity Index (DSI), terrestrial and groundwater storage anomalies from the Gravity Recovery and Climate Experiment (GRACE) satellites, groundwater well, and streamflow anomalies. Moreover, we identify the three major droughts with the highest severity (based on IDI) that occurred in 1965, 1987, and 2002 in the Sabarmati river basin. The three most severe droughts occurred in 1966, 1979, and 2010 in the Brahmani basin. Notwithstanding the large intermodel uncertainty, which arises primarily from precipitation projections, the drought frequency based on IDI is projected to decline in Sabarmati while it increases in Brahmani basin under the warming climate. Our results show that IDI can be effectively used for drought monitoring and assessment under retrospective and future climate in India.

1. Introduction

Drought is one of the most complex natural disasters, which is difficult to define (Lloyd-Hughes, 2014; Van Loon, 2015; Wilhite & Glantz, 1985). Drought can be related to a deficiency in rainfall, soil moisture, streamflow, the greenness of vegetation, and socioeconomic conditions (Mishra & Singh, 2010; Wilhite & Glantz, 1985; Zargar et al., 2011). Drought causes significant water and food insecurity, leading to economic losses and financial risks in developing countries like India (Godfray et al., 2010; Wilhite, 2005). Droughts (meteorological, hydrological, and agricultural) pose enormous challenges for drinking and irrigation water supply and also affect the economy of India, where more than 68% of people are dependent upon agriculture. Moreover, about 18% of India's total area is drought-prone, and about 50 million people are annually affected by drought (Dutta et al., 2013). India faces droughts due to poor summer monsoon caused by natural climate variability or climate change (Mishra et al., 2012; Koll Roxy et al., 2015). The positive phase of El Niño–Southern Oscillation (ENSO) has a considerable impact on the occurrence of drought in India. For instance, 11 out of 21 droughts were caused in El Niño years from 1871 to 1988 (WMO Switzerland, 1999).

Drought, in general, can be classified into four major categories—meteorological, hydrological, agricultural, and socioeconomic droughts (Mishra & Singh, 2010; Wilhite & Glantz, 1985). Meteorological drought occurs due to a deficiency in precipitation while hydrological drought is due to a shortage in streamflow, groundwater, or total water storage. Soil moisture deficit is a primary driver for agricultural drought (Mishra et al., 2018; Sheffield et al., 2004). However, water supply, demands, and other social responses can lead to socioeconomic drought (Van Loon, 2015; Wilhite, 2005). In addition to the drought types, droughts can also be characterized based on severity, intensity, duration, and areal extent (Mishra et al., 2016; Mishra & Singh, 2010). Therefore, an efficient drought monitoring system (Shah & Mishra, 2015) that integrates multiple aspects (types and characteristics) of droughts is necessary for adaptation and mitigation in India (Aadhar & Mishra, 2017; Shah & Mishra, 2015).

There are several indices for the monitoring and assessment of droughts (AghaKouchak et al., 2015; Mishra & Singh, 2010; Zargar et al., 2011). Standardized Precipitation Index (SPI; McKee et al., 1993) and Palmer Drought Severity Index (PDSI; Palmer, 1965) are the two most commonly used precipitation-based indices to monitor meteorological drought. Standardized Runoff Index (SRI) considers drought based on runoff or streamflow and can be useful for the drought monitoring in the snow-dominated basins (Shukla & Wood, 2008). Standardized Soil moisture Index (SSI; Hao & AghaKouchak, 2013) and the soil moisture percentile (Sheffield et al., 2004; Wang & Qu, 2009) are the most widely used indices for agricultural droughts (Mishra et al., 2018; Mishra et al., 2019). Apart from meteorological and hydrological drought indices, drought indices based on Normalized Difference Vegetation Index (NDVI; Ji & Peters, 2003), Vegetation Condition Index (VCI; Liu & Kogan, 1996), Drought Severity Index (DSI; Mu et al., 2013), Vegetation Temperature Condition Index (VTCI; Wan et al., 2004), and Standardized Precipitation Evapotranspiration Index (SPEI; Vicente-Serrano et al., 2010) are commonly used for agricultural drought monitoring. Groundwater drought can be measured using the long-term groundwater well observations or satellite data from Gravity Recovery and Climate Experiment (GRACE; <https://grace.jpl.nasa.gov/data/get-data/>; Kumar et al., 2016; Sinha et al., 2017; Thomas & Famiglietti, 2019).

The most common drought indicators (SPI, PDSI, and SPEI) often do not include groundwater for drought monitoring and assessment primarily because of the lack of groundwater observations (Thomas et al., 2017). Including groundwater response in drought monitoring and assessment in India is essential due to the rapid depletion of groundwater (Asoka et al., 2017; Chen et al., 2016; Long et al., 2016; Rodell et al., 2009; Tiwari et al., 2009). Moreover, groundwater remains the primary source of irrigation (Mishra et al., 2018) and drinking water. Notwithstanding, the previous developments of drought monitoring systems in India (Aadhar & Mishra, 2017; Shah & Mishra, 2015) and South Asia (https://sites.google.com/a/iitgn.ac.in/high_resolution_south_asia_drought_monitor/), the response of groundwater during drought remains excluded. Monitoring of groundwater drought using land surface hydrological models can be a valuable alternative to the lack of in situ measurements of groundwater (Li & Rodell, 2015). There have been efforts to model groundwater variability for drought assessment; however, the assessment in India has been lacking. For instance, Kumar et al. (2016) and Van Loon et al. (2017) evaluated the use of SPI as a groundwater drought indicator in Germany. Thomas et al. (2017) used a groundwater drought index based on the GRACE satellites to identify the role of human and climate systems on groundwater depletion in California. Moreover, Castle et al. (2014) reported that during the persistent droughts groundwater depletion can be significant, which, in turn can affect the water security. Therefore, we identify that there is a strong need to include groundwater storage variability in the drought monitoring and assessment in India.

Copulas have been used for multivariate hydrological analysis including rainfall (De Michele & Salvadori, 2003; Grimaldi & Serinaldi, 2006; Kao & Govindaraju, 2007; Kuhn et al., 2007; Zhang & Singh, 2007) and flood frequency analysis (Favre et al., 2004; Renard & Lang, 2007; Shiau et al., 2006; Wang et al., 2009; Zhang & Singh, 2006). The use of copula for development of joint drought index and frequency analysis is also not uncommon (Beersma & Buishand, 2004; Hao & Singh, 2015; Kao & Govindaraju, 2010; Liu et al., 2016; Saghafian & Mehdikhani, 2014; Shiau, 2006; Song & Singh, 2010). The concept of copula has been used for the development of multivariate drought indices (Hao & AghaKouchak, 2013; Ma et al., 2014). Chang et al. (2016) used Precipitation Anomaly Percentage, Runoff Anomaly Percentage, SPI, and Modified Palmer Drought Severity Index to develop copula-based integrated drought index. However, the integration of groundwater for overall drought characterization remains largely unexplored, especially in India, where groundwater is considered as a lifeline for food and fresh water security (Mishra et al., 2018).

While hydrological and meteorological indicators for drought monitoring and assessment provide the information on drought, using multiple indices for drought assessment remains a challenge due to lack of long-term in situ observations. Drought monitoring and declaration in India has been a great challenge due to the lack of near-real-time observations and the complexity associated with the drought declaration methodology. Recently, the National Disaster Management Authority (NDMA: <http://agricoop.nic.in/sites/default/files/Manual%20Drought%202016.pdf>) of India developed the drought manual to identify the onset and recovery of drought. However, there are operational challenges for the drought management of India due to difficulty in drought declaration. The difficulty of identifying the drought onset or drought declaration is primarily due to the number of indicators that have been suggested in the drought manual for drought declaration. In addition, the lack of real-time groundwater observations makes it difficult to assess the

role of groundwater in drought or the impacts of groundwater on drought. The indicators suggested by the drought manual are not readily available to the state governments nor they are available for long enough to estimate their departure from normal. Considering these challenges, the present study offers two novel insights that can be valuable for drought monitoring and assessment in India: (i) inclusion of the response of groundwater for drought monitoring, and (ii) combining the number of indicators that represent meteorological, hydrological, and agricultural drought to a single Integrated Drought Index (IDI). The development of IDI can provide timely information to the stakeholders (farmers, state government, and water managers) for drought onset and recovery. The real-time meteorological data are currently being used in our ongoing efforts in the South Asia drought monitoring system (https://sites.google.com/a/iitgn.ac.in/high_resolution_south_asia_drought_monitor/), which provides us a basis to include the framework based on IDI for drought monitoring in India.

2. Data and Methods

2.1. Data

We used 0.25° daily gridded precipitation, maximum and minimum temperatures (1951–2017) from the India Meteorological Department (IMD; Pai et al., 2015; Srivastava et al., 2009). Pai et al. (2015) used the inverse distance weighting (IDW) interpolation scheme (Shepard, 1984) to develop gridded precipitation product using data from 6,995 observational stations located across India. Climatological features and spatial variability in Indian summer monsoon are well captured in the gridded precipitation (Pai et al., 2015). Daily maximum and minimum temperatures at 1° were developed using the data of 395 observational stations across India (Srivastava et al., 2009), which were further regridded to 0.25° using synergic mapping and temperature lapse rate using the methodology described in Maurer et al. (2002). Observed gridded precipitation and temperature data sets have been used in many previous studies on droughts and heat waves (Shah et al., 2016a, 2016ab; Mishra et al., 2018; Mishra et al., 2014; Kumar & Mishra, 2019). We used observed streamflow from India Water Resources Information System (India-WRIS) to evaluate the performance of the hydrological model. The streamflow gauge stations were selected based on the availability of the long-term continuous data and the minimal influence of reservoir operations. Therefore, we do not consider the role of irrigation and reservoirs in our simulations.

We obtained Terrestrial Water Storage (TWS) data from the GRACE satellite (<ftp://podaac-ftp.jpl.nasa.gov/allData/tellus/L3/landmass/RL05>; accessed on 2nd April 2019), which is available for the 2002–2016 period at 1° spatial resolution. Monthly standardized TWS anomalies were constructed by removing the average TWS for 2002–2016 from monthly TWS and dividing it with a standard deviation of each month. Groundwater storage anomalies from the GRACE TWS were estimated after removing surface water (soil moisture, canopy water, and snow water equivalent). Surface water data were obtained from the three (VIC, Noah, and CLM) land surface models that were the part of Global Land Data Assimilation System (GLDAS, <https://disc.gsfc.nasa.gov/services/grads-gds/gldas>; accessed on 2nd April 2019; Rodell et al., 2004). Further details on GRACE TWS and groundwater anomalies can be obtained from Asoka et al. (2017, 2018). In addition to groundwater storage anomalies from the GRACE satellites, we obtained groundwater well observations from the observational wells across India that are available for January, May, August, and November (1996–2016) from the Central Groundwater Board (CGWB). Drought Severity Index (DSI) data were obtained at 0.05° spatial resolution for the period of 2001–2011, which were developed using MODIS evapotranspiration and Normalized Difference Vegetation Index (NDVI) as described in Mu et al. (2013).

We obtained daily precipitation, maximum and minimum temperatures from eight general circulation models (GCMs: BNU-ESM, CESM1-CAM5, GFDL-ESM 2M, MPI-ESM-LR, NorESM1-M, GFDL-ESM 2G, MIROC-ESM, and MIROC-ESM-CHEM) that participated in the Coupled Model Intercomparison Project Phase 5 (CMIP5; Taylor et al., 2012). We note that the selected eight GCMs may not cover the full range of uncertainty (McSweeney & Jones, 2016); however, our choice of GCMs is limited by their performance. The selected eight GCMs were evaluated extensively for their performance to capture the observed features related to the summer monsoon (Ashfaq et al., 2017). Ashfaq et al. (2017) reported that these GCMs perform well to simulate the key features of the summer monsoon precipitation, temperature, and associated intra-seasonal variability in South Asia. We obtained the climate data for the historical (1951–2006) and future

(2006–2100) periods for the two Representative Concentration Pathways (RCPs) including RCP 2.6 (low emission scenario) and RCP 8.5 (high emission scenario; Moss et al., 2010). Moreover, we further down-scaled and bias corrected the precipitation and temperatures data at 0.25° using trend preserving bias correction approach, which has been widely used (Haddeland et al., 2014; Schewe et al., 2014; van Vliet et al., 2016) in the Intersectoral Model Intercomparison Project (ISIMIP, Hempel et al., 2013).

2.2. Study Area

We selected two basins to test the applicability of IDI in India. Sabarmati River Basin (SRB) is located in the arid and semiarid zone of western India, which drains into the Arabian Sea. On the other hand, Brahmani River Basin (BRB) is located in the tropical-subtropical region and drains into the Bay of Bengal (Figure 1). The SRB extends over states of Gujarat and Rajasthan with an approximate area of 21,674 km² and lies between 70.97° and 73.85° east longitudes and 22.25° to 24.78° north latitudes. The average annual precipitation in SRB is about 787.5 mm. Brahmani is a major interstate east flowing river among the peninsular rivers in India. BRB lies between 20.46° and 23.58° north latitude and 83.86° to 87.05° east longitude and extends over Jharkhand, Chhattisgarh, and Orissa with a drainage area of 39,033 km². The average annual precipitation in BRB is about 1,460 mm. Dharoi and Rengali are the two major reservoirs in SRB and BRB, respectively. The basic information about climatic zones in India (Kottek et al., 2006), topography, land use/land cover (LULC), and major observation stations of SRB and BRB is presented in Figure 1.

2.3. The VIC-SIMGM Model

We used Variable Infiltration Capacity (VIC: Cherkauer et al., 2003; Gao et al., 2009; Liang et al., 1994, 1996) with SIMple Groundwater Model (SIMGM: Rosenberg et al., 2013; Niu et al., 2007) to simulate hydrological variables. The VIC model is a macroscale semidistributed grid-based hydrological model, which simulates water and energy fluxes in each grid at daily to subdaily time scales. The VIC model differs from other land surface models in the parameterization of subgrid variability in vegetation, land cover, and soil moisture (Gao et al., 2009). Vegetation parameters, soil parameters, and climatic forcing (consisting of precipitation, maximum and minimum temperature, and wind speed) are the primary inputs to the VIC model. We used vegetation parameters from the Advanced Very High-Resolution Radiometer (AVHRR) global land-cover information (Hansen et al., 2000; Sheffield & Wood, 2007). We developed soil parameters using the data from the Harmonized World Soil Database (HWSD). The additional parameters related to SIMGM including maximum subsurface flow, specific yield, decay factor, and initial water table depth were obtained or adjusted as described in Niu et al. (2007) and Rosenberg et al. (2013).

In SIMGM, groundwater is parameterized as a lumped, unconfined aquifer beneath the soil layers as in other models (Gedney et al., 2003; Yeh et al., 2005). Groundwater discharge (Q_d) is parameterized as an exponential function of the water table depth (equation (1)) while groundwater recharge (Q_r) is parameterized by Darcy's law (equation (2)).

$$Q_d = Q_{d\max} * e^{-fZV} \quad (1)$$

Where $Q_{d\max}$ is the maximum groundwater discharge when the water table depth is zero, ZV is the water table depth, and f is the decay factor.

$$Q_r = -K_a \frac{-Z\nabla - (\varphi_{bot} - Z_{bot})}{(Z\nabla - Z_{bot})} \quad (2)$$

where K_a is hydraulic conductivity, Z_{bot} is the depth to the bottom of the soil column, and φ_{bot} is the matric potential of the bottom soil layer. Temporal change of an unconfined aquifer storage $\frac{dW_a}{dt}$ is equal to the difference of aquifer recharge and discharge ($Q_r - Q_d$). Rosenberg et al. (2013) added a lumped, unconfined aquifer beneath the lowest (third) soil layer and replaced the baseflow scheme of the VIC model with that of SIMGM (equation (1)). Surface runoff parameterization in the VIC-SIMGM is similar to that of the VIC model. Simulated runoff and baseflow from each grid were routed using a standalone routing model, which is based on the unit hydrograph method (Lohmann et al., 1996, 1998). The major limitation of the SIMGM is the lack of a direct connection between surface water and groundwater in its parameterization (Rosenberg

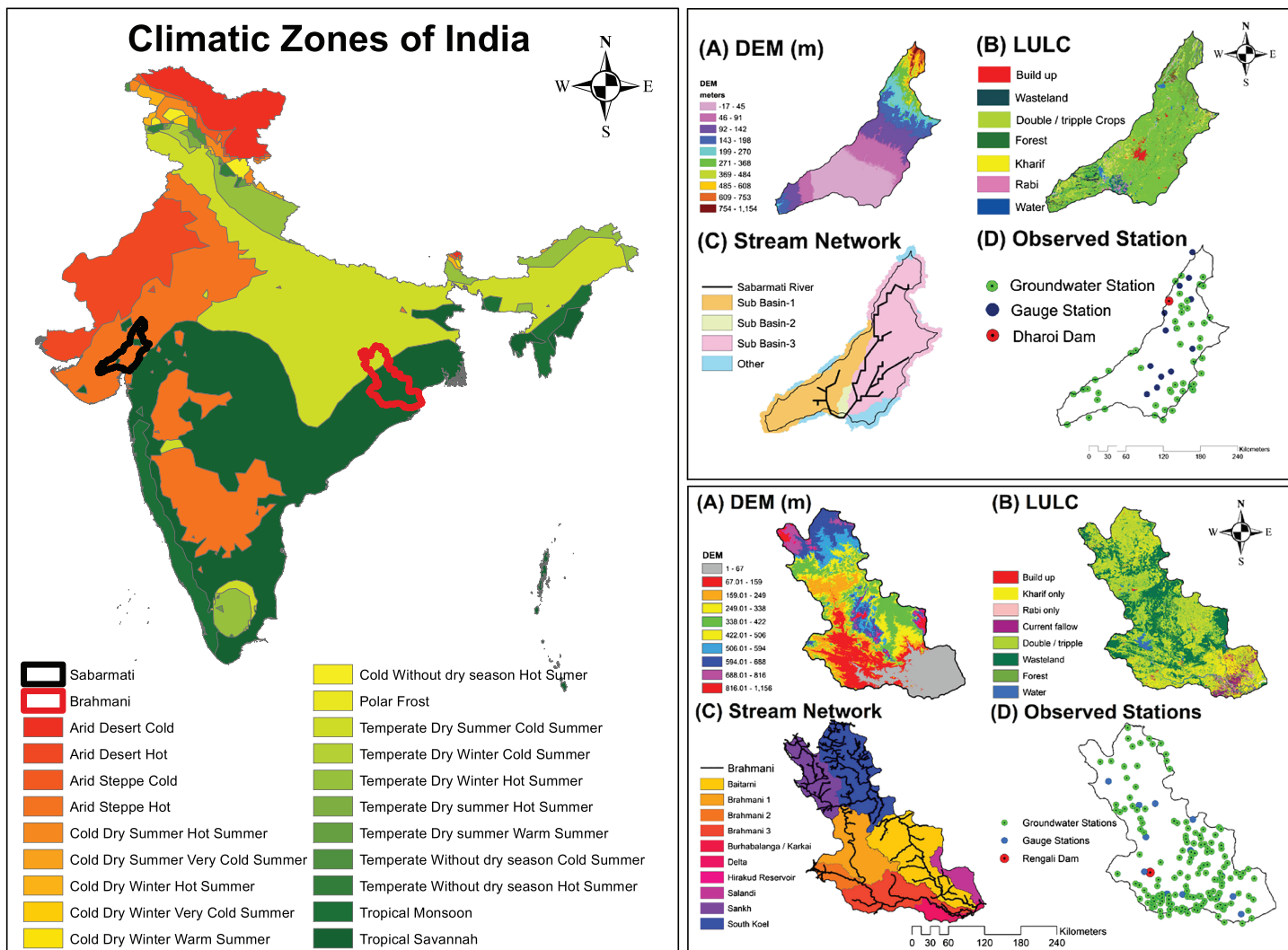


Figure 1. Climatic zones of India. Basic information related to topography (A), land use/land cover (B), stream network(C), and groundwater, streamflow observation stations and dams (D) for Sabarmati and Brahmani River Basins.

et al., 2013). Moreover, as the VIC model is applied at 0.25° spatial resolution, the horizontal transfer of water from one grid to another was assumed to be negligible. The VIC-SIMGM does not consider the influence of the pumping, which is a major driver of groundwater storage variability in the highly irrigated basins in India (Asoka et al., 2017; Rodell et al., 2009; Tiwari et al., 2009). Considering this limitation, our aim here is to simulate the groundwater storage affected by the year-to-year variability in climate instead of human influence. Simulated hydrologic variables from the VIC-SIMGM were used to develop and test IDI in the two basins located in a diverse climate in India.

We manually calibrated the VIC-SIMGM against monthly observed streamflow at the Jotasun and Kheroj upstream of Dharoi dam in the Sabarmati river basin (Figure 2) and at Gomlai in Brahmani river basin (Figure 3). We used nine parameters of the VIC-SIMGM to manually calibrate the model against observed streamflow and standardized groundwater depth anomaly (estimated using CGWB well data). More details of the calibration parameters (infiltration parameter (B_{inf}), soil layer thickness (second and third layers), maximum baseflow velocity (D_{smax}), the fraction of maximum soil moisture content (W_s), the fraction of maximum baseflow velocity (D_s), specific yield of an aquifer, maximum subsurface baseflow, and decay factor with their ranges can be obtained from Mishra et al., (2010), Shah et al. (2016b), Niu et al. (2007), and Rosenberg et al. (2013).

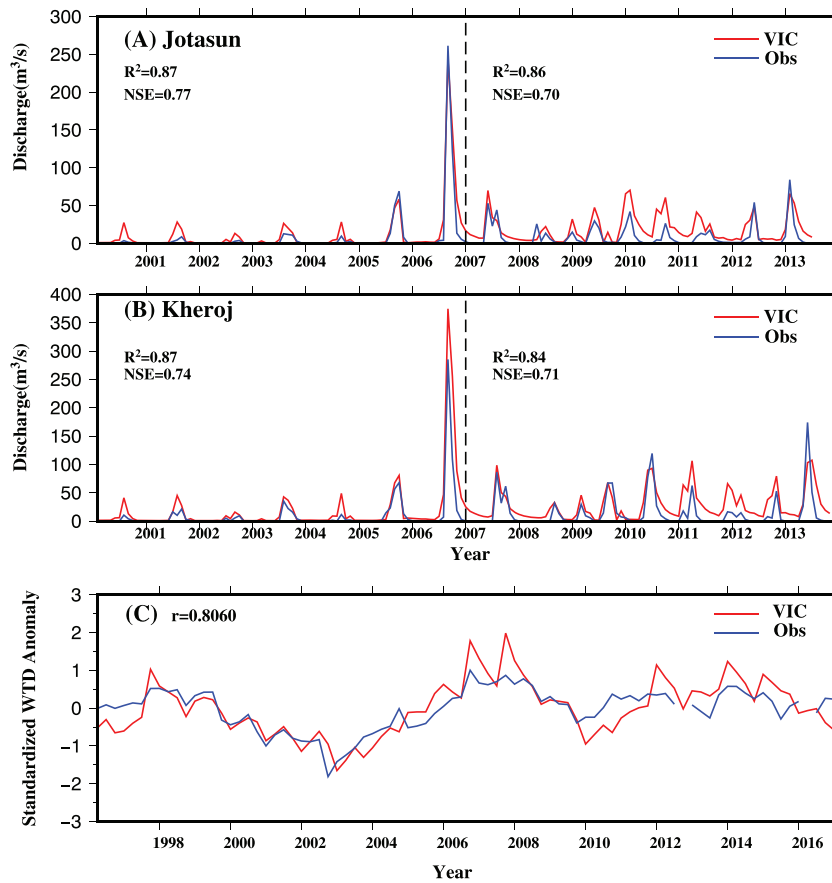


Figure 2. (A, B) Comparison of monthly observed (m^3/s ; blue) and VIC-SIMGM simulated streamflow (red) at two locations in the Sabarmati River Basin; Jotasun and Kheroj, respectively. The dotted line separates the calibration (2000–2007) and evaluation (2008–2014) periods based on the availability of observed data. (C) Comparison of standardized observed basin averaged groundwater depth anomaly (based on CGWB data; blue) and VIC-SIMGM simulated groundwater depth anomaly (red) for Sabarmati River Basin (1996–2016; Jan-May-Aug-Nov).

2.4. Development of IDI

We used copula to develop IDI, which integrates meteorological, hydrological, and agricultural droughts and associated indices (SPI, SSI, SRI, and SGI). Hao and AghaKouchak (2013) used the concept of copula to develop a Multivariate Standardized Drought Index (MSDI) using precipitation and soil moisture at different time scales. Since our aim is to integrate meteorological, hydrological, and agricultural droughts, we use four indices: 12-month SPI (meteorological drought), 1-month SSI (agricultural drought), 4-month SRI and 1-month SGI (hydrological drought) to develop IDI. These standardized indices were estimated using the methodology for SPI as described in McKee et al. (1993). Precipitation has a strong seasonality in India, with more than 80% of the total annual rainfall occurring during the four monsoon months (June–September; Mishra et al., 2012; Rana et al., 2015). Therefore, to account for the precipitation seasonality, we consider 12-month SPI that represents 12-month cumulative precipitation to develop IDI. Since we use 1-month SSI, the short-term variability of precipitation can be accounted in SSI.

To take into account the drought propagation from meteorological to hydrological, we evaluated the correlation between 12-month SPI with SSI, SRI, and SGI of different time scales as well as at a time lag of 1 to 19 months (Tables S1–S3 in the supporting information). Our analysis shows that 12-month SPI is the best correlated with 1-month SSI, 1-month SGI, and 4-month SRI (Tables S1–S3). The use of 1 month SGI and SSI is justified due to the high persistence in soil moisture (60 cm to represent root zone as in Mishra et al., 2018) and groundwater at the lag of 4 months in Sabarmati River basin. However, we find low persistence at the lag of 4 months in the Brahmani River basin as it is located in the humid or tropical region. Moreover, 4-month SRI is used, as a 4-month deficit in total runoff or streamflow is a good indicator of hydrological drought

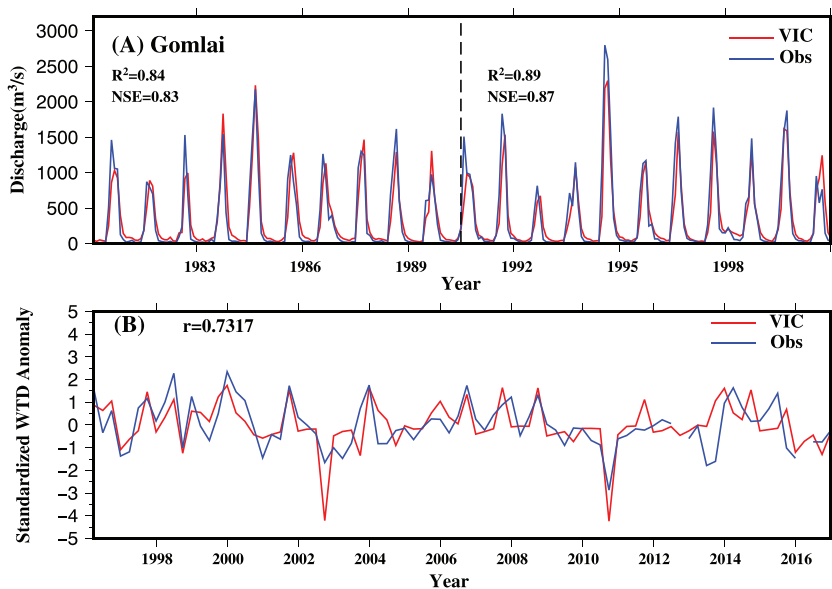


Figure 3. (A) Comparison of monthly observed (m^3/s ; blue) and VIC-SIMGM simulated monthly streamflow (red) at Gomlai in Brahmani River Basin. The dotted line separates the calibration (1981–1990) and evaluation (1991–2000) periods based on the availability of observed data. (B) Comparison of standardized observed (based on CGWB data; blue) and VIC-SIMGM simulated groundwater depth anomalies (red) for Brahmani River Basin (1996–2016; Jan-May-Aug-Nov).

(Shukla & Wood, 2008). Since there may be a lag between meteorological, hydrological, and agricultural droughts (Apurv et al., 2017), the selection of different accumulation periods for SSI (1 month), SRI (4 month), and SGI (1 month) can account for the influence of time lag. We considered the accumulation periods for SSI, SGI, and SRI that provided us the best correlation against the 12-month SPI at zero lag (Tables S1–S3).

Apart from the selected time periods of SPI (12 months), SRI (4 months), SSI (1 month), and SGI (1 month), we estimated IDI using different combinations of SPI (1, 3, 6, and 9 months), 1-month SSI, 1-month SGI, and 4-month SRI to see if the proposed IDI is able to capture both short- and long-term droughts. We estimated the onset and termination of droughts (explained in the characterization of drought section) for different IDI estimates for the drought of 1999–2005 (Figures S1 and S2). We find that the onset of the drought is almost the same for different IDI while the termination is delayed by 9 to 10 months in the proposed IDI based on 12-month SPI. This delayed termination can be attributed to long-term (12-month) precipitation considered for IDI. However, the delayed termination in the proposed IDI provides a more conservative estimate of drought duration. Therefore, the proposed IDI based on 12-month precipitation can account for both short- and long-term drought variability. We evaluated the correlation between the proposed IDI with all other IDI estimates, which show a strong relationship with the other estimates of IDI based on SPI at 1, 3, 6, and 9 months (Figure S3).

We used copula to integrate the response of SPI, SRI, SSI, and SGI in drought using IDI. Copulas are used to derive joint distribution of two or more variables, regardless of their original marginal distribution. There are many copula families available, which have been used for joint bivariate distribution (Hao & AghaKouchak, 2013; Kao & Govindaraju, 2010; Keyantash et al., 2002). Though the applicability of copula for more than two variables has its own limitation, we used the Gaussian copula to fit the joint distribution for four variables. Generally, there are two types (“t copula” and “Gaussian copula”) of copulas that are used to fit the distribution with four or more variables (Ma et al., 2014). Ma et al. (2014) reported that many copulas that perform well for bivariate problems (e.g., Archimedean copulas) are not suitable for higher-order spaces while metaelliptical copulas (Gaussian copula and Student's *t* copula based on multivariate Student's *t* distribution) can be useful for large dimensions. Assuming, 12-month SPI (A), 1-month SSI (B), 4-month SRI (C), and 1-month SGI (D) as random Gaussian variables, the joint distribution with joint cumulative probability “*p*” can be expressed as (Sklar, 1959)

Table 1*Reconstruction of Major Droughts (Duration \geq 6 Months) and Their Characteristics Based on 1-Month IDI During 1952–2017 for the Sabarmati River Basin*

Onset year	Onset month	Termination year	Termination month	Duration (months)	Max intensity	Average intensity	% area IDI	% area SPI	% area SSI	% area SRI	% area SGI	Severity score
1952	1	1953	9	20	-2.31	-0.82	100	100	100	98	74	16.47
1960	9	1961	9	12	-1.07	-0.51	72	84	81	77	51	4.42
1963	5	1963	11	6	-0.52	-0.17	60	53	44	81	56	0.61
1964	8	1970	9	73	-1.70	-0.88	100	100	93	100	95	64.01
1972	6	1973	9	15	-2.10	-1.32	100	100	100	100	81	19.83
1974	8	1975	10	14	-2.04	-1.15	100	100	100	100	65	16.07
1979	8	1981	8	24	-0.87	-0.31	40	84	63	72	33	2.94
1982	9	1983	5	8	-0.66	-0.11	49	70	72	84	35	0.44
1985	7	1990	9	62	-3.34	-1.02	100	100	100	100	100	63.15
1993	9	1994	7	10	-1.01	-0.16	51	30	58	70	53	0.80
1995	9	1997	5	20	-0.64	-0.17	65	91	58	95	47	2.15
1999	8	2005	7	71	-2.49	-0.86	100	100	100	100	98	61.00
2008	7	2010	8	25	-1.39	-0.50	74	91	74	86	53	9.31
2016	1	2016	8	7	-0.65	-0.28	74	95	70	65	12	1.44

$$P(A \leq a, B \leq b, C \leq c, D \leq d) = C_p[F(A), F(B), F(C), F(D)] = p \quad (3)$$

Where C_p represents Gaussian copula and $F(A), F(B), F(C), F(D)$ are the empirical cumulative distribution function of 12-month SPI, 1-month SSI, 4-month SRI, and 1-month SGI, respectively. IDI can be estimated by taking the inverse of joint cumulative probability (p) as

$$IDI = \varphi^{-1}(p) \quad (4)$$

where φ is the standard normal distribution function.

We used Cramer-von-Mises statistic (S_n) and Kolmogorov-Smirnov statistic (T_n) statistics as goodness-of-fit measures to select an appropriate copula (Genest et al., 2006; Genest & Favre, 2007). These statistical measures (S_n and T_n) have been used for estimating the goodness of fit of a proposed cumulative distribution function to a given empirical distribution function. The p -values of statistic S_n and T_n are presented in (Figures S4 and S5 and Tables S4 and S5). Copula cannot be rejected if the corresponding p -value from Cramer-von-Mises statistic (S_n) and Kolmogorov-Smirnov statistic (T_n) is more than 0.05 or at 5% significance level. We compared p -values for both the copula cases (spatially and temporally using the monthly

Table 2*Reconstruction of Major Droughts (Duration \geq 6 Months) and Their Characteristics Based on 1-Month IDI During 1952–2017 for the Brahmani River Basin*

Onset year	Onset month	Termination year	Termination month	Duration (months)	Max intensity	Average intensity	% area IDI	% area SPI	% area SSI	% area SRI	% area SGI	Severity score
1954	2	1955	10	20	-1.83	-0.67	95.77	95.77	88.73	95.77	90.14	12.88
1957	6	1958	10	16	-1.16	-0.66	97.18	90.14	100.00	94.37	92.96	10.27
1962	6	1963	7	13	-1.58	-0.89	78.87	87.32	74.65	90.14	78.87	9.12
1965	5	1971	4	71	-1.48	-0.48	98.59	97.18	100.00	95.77	95.77	33.36
1972	5	1973	8	15	-0.82	-0.38	71.83	83.10	95.77	85.92	74.65	4.10
1974	6	1975	8	14	-1.22	-0.68	91.55	94.37	98.59	95.77	74.65	8.73
1976	6	1977	6	12	-1.06	-0.65	80.28	80.28	85.92	94.37	84.51	6.29
1979	5	1981	3	22	-2.08	-0.88	100.00	100.00	100.00	100.00	100.00	19.37
1981	9	1983	9	24	-1.54	-0.52	100.00	88.73	100.00	100.00	100.00	12.39
1984	10	1985	8	10	-0.67	-0.21	70.42	30.99	81.69	84.51	92.96	1.49
1987	6	1990	3	33	-1.28	-0.26	98.59	76.06	100.00	100.00	88.73	8.55
1992	6	1993	7	13	-1.13	-0.66	88.73	73.24	98.59	100.00	92.96	7.65
1996	8	1997	7	11	-1.35	-0.85	88.73	66.20	92.96	97.18	88.73	8.30
2000	8	2003	10	38	-1.81	-0.45	91.55	92.96	87.32	95.77	92.96	15.61
2004	9	2005	10	13	-0.45	-0.15	45.07	56.34	78.87	52.11	45.07	0.86
2008	11	2011	6	31	-2.01	-0.66	94.37	97.18	95.77	98.59	92.96	19.29

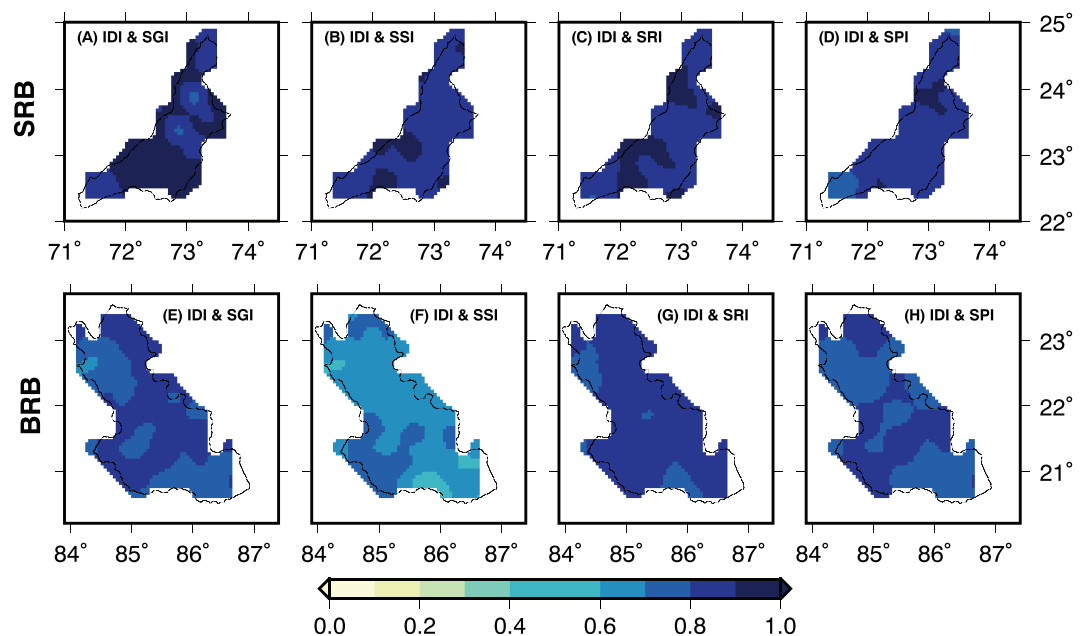


Figure 4. (A–D) Correlation of IDI (1952–2017) with 1-month SGI, 1-month SSI, 4-month SRI, and 12-month SPI, respectively, for Sabarmati River Basin; (E–H) correlation of IDI (1952–2017) with 1-month SGI, 1-month SSI, 4-month SRI, and 12-month SPI, respectively, for Brahmani River Basin for the 1952–2017 period.

data from 1952–2017) and found the use of the Gaussian copula is more reliable than *t* copula. Gaussian copula shows higher *p*-value (Tables S4 and S5) and also the area where the copula fails (*p*-values smaller than 0.05) is less in the case of Gaussian copula (Figure S4 and S5).

2.5. Characterization of Drought

We characterized the major retrospective droughts during 1952–2017 using IDI for both the basins. We use onset, termination, duration, maximum and mean intensity, and the areal extent to characterize droughts. The onset and termination of a drought are probably the two most complex issues in drought monitoring due to spatial and temporal variability in precipitation, runoff, groundwater, and soil moisture (Shukla et al., 2011). Drought onset was defined as the first month for which IDI is negative and remains negative consecutively for 3 months as in Mo (2011). Similarly, drought termination was identified as the first month for which IDI is positive and stays positive for at least three consecutive months. Drought duration was defined as the number of months between the onset and termination. We identify all the drought spells during 1952–2017 with the duration of six or more months. Two neighboring drought spells were merged if the termination was not found for the previous drought and onset started for the next drought. Therefore, if the interdrought duration was less than 3 months, the two drought spells were merged and considered as a single drought spell. We estimated the percentage area affected by droughts by taking the ratio of total grids with IDI less than −0.8 (Tables 1 and 2) to the total number of grids in a basin. We identified different categories (abnormally dry, moderate, severe, extreme, and exceptional) based on the IDI ranges (Table S6) as described in Svoboda et al. (2002).

3. Results

3.1. Performance of the VIC-SIMGM

The VIC-SIMGM was manually calibrated against the observed monthly streamflow and groundwater table anomalies in both the basins (Figures 2 and 3). The VIC-SIMGM performs well in capturing temporal variability of monthly streamflow for the calibration and evaluation periods. Nash-Sutcliffe Efficiency (NSE: Nash & Sutcliffe, 1970) and coefficient of determination (R^2) for the calibration period (2000–2007) for the Sabarmati River basin are 0.77 and 0.87, respectively, at Jotasun and 0.74 and 0.87 at Kheroj stations (Figure 2). Similarly, the VIC-SIMGM performs well with NSE and R^2 of 0.83 and 0.84, respectively, for

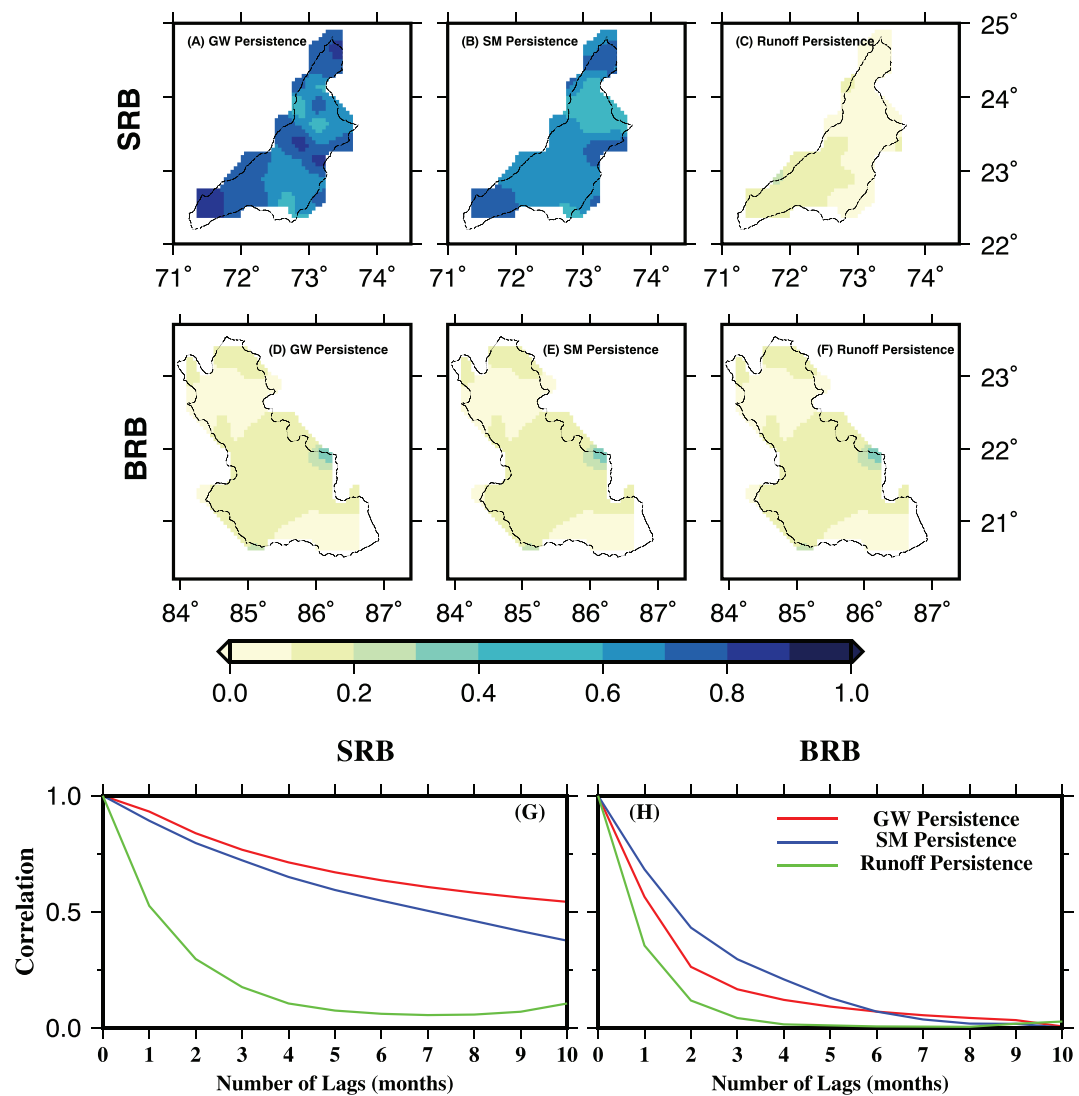


Figure 5. (A-C) Persistence of groundwater, soil moisture, and runoff at 4-month lag for Sabarmati River Basin and (D-F) Brahmani River Basin. (G, H) Autocorrelation function of soil moisture, groundwater, and runoff for Sabarmati and Brahmani River Basins for the period of 1952–2017.

the calibration period at Gomlai in the Brahmani basin (Figure 3). The VIC-SIMGM performs well for the evaluation periods for both the basins with NSE and R^2 higher than 0.7 and 0.8, respectively (Figures 2 and 3). We also compared basin averaged standardized groundwater table depth anomalies for both the basins. The calibrated and evaluated VIC-SIMGM performs well for groundwater table anomalies in both the basins with correlation coefficient (r) of 0.80 and 0.73, respectively, for SRB and BRB (Figures 2 and 3).

Observed groundwater table data from the central groundwater board (CGWB) is available only for the four (Jan, May, Aug, and Nov) months in each year for 1996–2016 for both basins (Figures 2 and 3). Due to large spatial variability in groundwater table in the basins (due to shallow and deep wells), we used basin-averaged standardized anomalies of groundwater table instead of absolute water table depth (Kumar et al., 2016). Since we calibrated both streamflow and groundwater anomalies together, the bias in modeled streamflow can be attributed to calibration parameters (Figures 2 and 3). Moreover, the calibration was performed manually, which does not consider the entire range of calibration parameters (Gupta et al., 1999). Despite these limitations, we find that the calibrated and evaluated VIC-SIMGM performs well for streamflow as well as groundwater variability in the two basins and simulated hydrologic variables can be used for

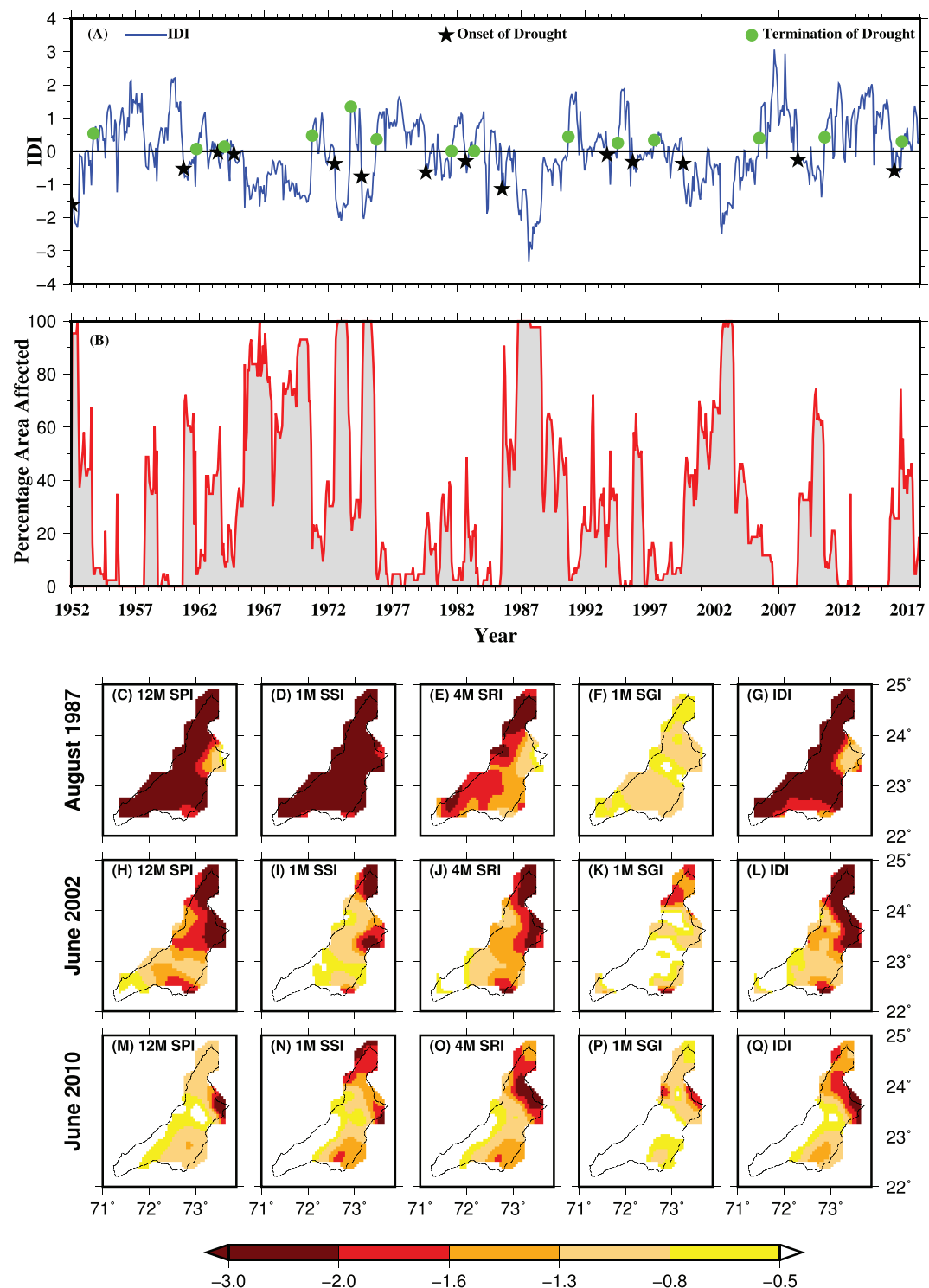


Figure 6. (A) One-month basin averaged IDI (1952–2017), (B) percentage area affected by droughts, (C, H, M) 12-month SPI, (D, I, N) 1-month SSI, (E, J, O) 4-month SRI, (F, K, P) 1-month SGI, (G, L, Q) 1-month IDI at the end of August 1987, June 2002, and June 2010, respectively, in the Sabarmati River Basin.

the development and evaluation of IDI. Moreover, the VIC model has been evaluated for the other hydrologic variables (ET, soil moisture) in India and previous studies found a satisfactory performance (Shah et al., 2016a, 2016b, 2019).

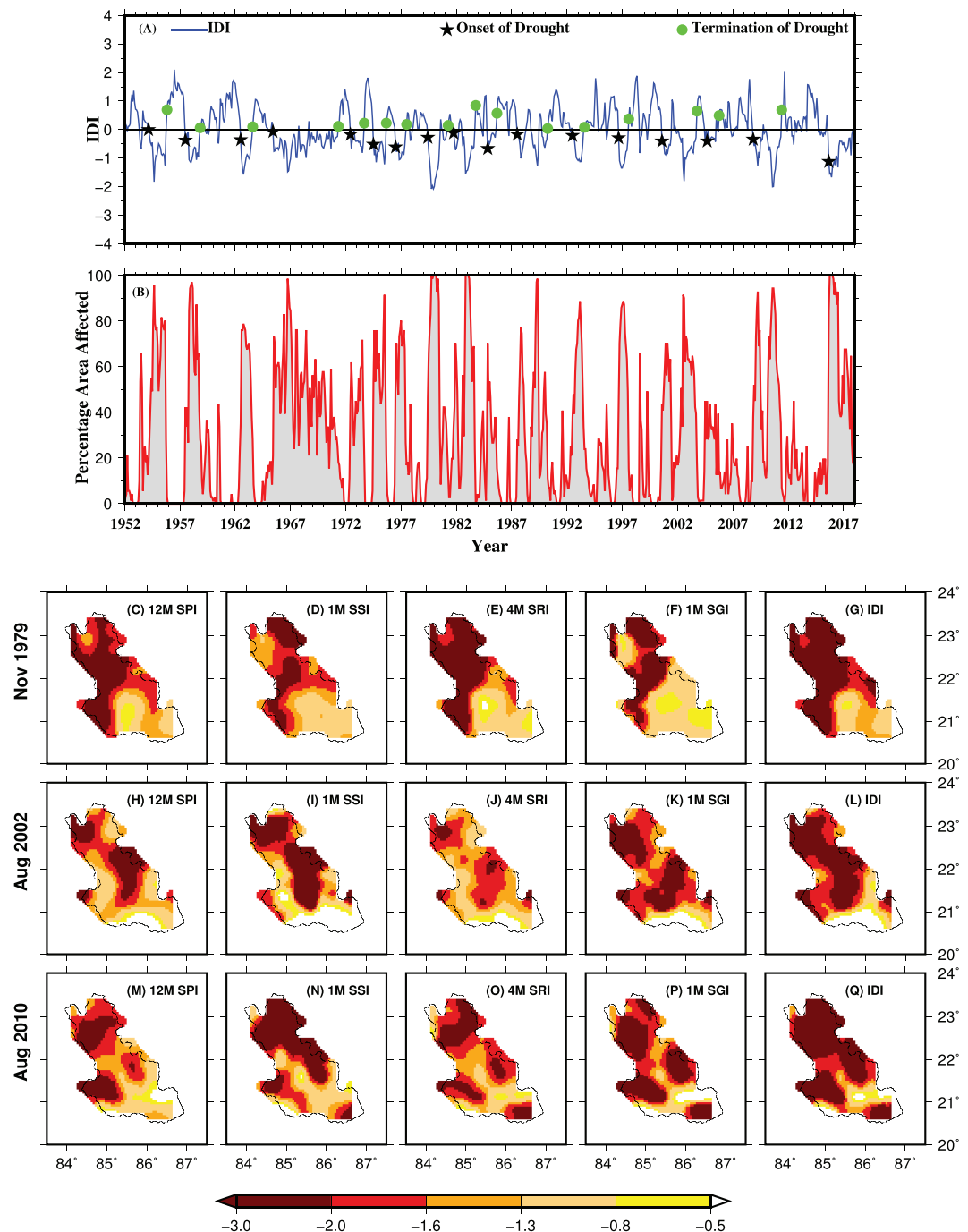


Figure 7. Same as Figure 6 but for the Brahmani River Basin.

3.2. Development of IDI

We estimated IDI using 12-month SPI, 1-month SSI, 4-month SRI, and 1-month SGI for both the river basins in India for 1952–2017. We estimated the correlation between monthly IDI with SGI (1 month), SSI (1 month), SRI (4 months), and SPI (12 months) to understand if the response of meteorological, hydrological, and agricultural droughts is well captured in IDI (Figure 4). We find that 1-month IDI is well correlated (correlation more than 0.8) with all the indicators in the Sabarmati river basin. However, we note that the correlations are slightly weaker in the Brahmani river basin than that of the Sabarmati river basin. In contrast to the Sabarmati river basin, the Brahmani basin is located in the humid and subhumid region and the mean

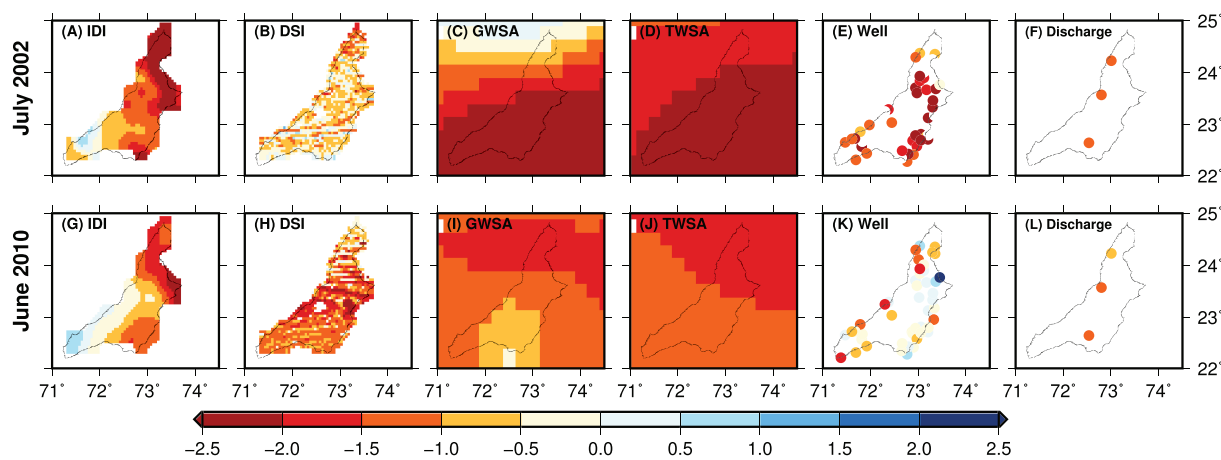


Figure 8. Evaluation of IDI against other observations for July 2002 and June 2010. (A, G) One-month IDI, (B, H) 1-month DSI, (C, I) GRACE-derived Groundwater Storage Anomaly (GWSA), (D, J) GRACE-derived Total Water Storage Anomaly (TWSA), (E, K) standardized observed groundwater depth anomaly from CGWB well data, (F, L) 4-month moving average streamflow anomaly (at three locations) at the end of July 2002 and June 2010 in Sabarmati River Basin.

annual precipitation is substantially higher than the Sabarmati basin, which is likely to be associated with lower soil moisture persistence in the Brahmani basin. To evaluate this, we estimated the persistence of soil moisture, groundwater, and runoff at the 4-month lag to understand spatial differences in these variables in the Sabarmati and Brahmani basin. We find that soil moisture and groundwater show a high persistence (correlation more than 0.4) at 4-month lag (Figure 5) in SRB and low persistence in BRB, which is due to the higher precipitation regime of eastern India. On the other hand, total runoff shows a substantially lower persistence in comparison to soil moisture and groundwater in both the basins. Therefore, we used 4-month SRI while 1-month SSI and SGI for estimation of IDI, which is consistent with the correlation analysis (Tables S1–S3).

After the estimation of IDI for both the basins, we identified drought spells and characteristics using basin averaged IDI for the period of 1952–2017 (Figures 6 and 7). We identified 14 major drought spells with duration more than or equal to 6 months that occurred in the Sabarmati River basin during 1952–2017 (Figure 6). We estimated overall severity score as the multiplication of duration (months), average intensity, and peak fractional areal extent for each drought spell to combine the influence of the drought characteristics. Based on the overall severity score, the most severe droughts in SRB occurred in 1965, 1987, and 2002 (Table 1). The 1965 drought started in August 1964 and terminated in September 1970 with a duration of 73 months. This was the longest drought that occurred in SRB during 1952–2017 with average and peak intensities of −0.88 and −1.7, respectively (Table 1). The next most severe drought (based on IDI) started in July 1985 and

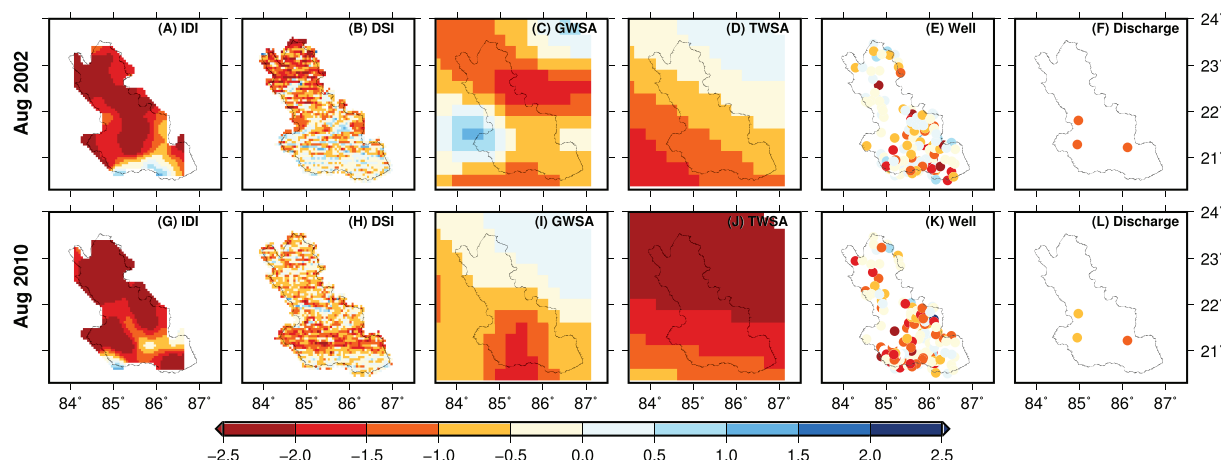


Figure 9. Same as Figure 8 but for the Brahmani River Basin.

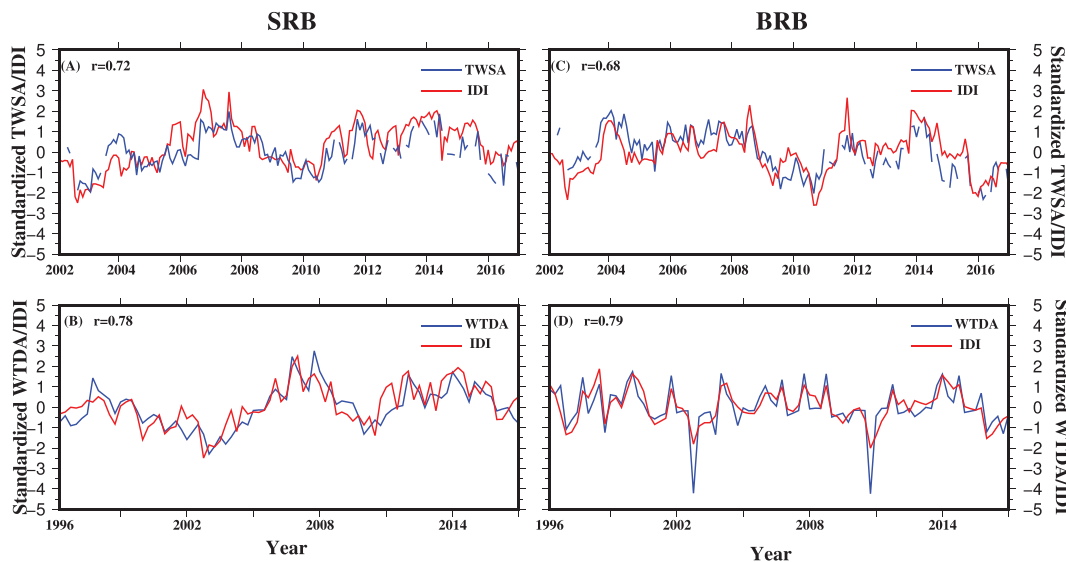


Figure 10. (A, C) Comparison of 1-month IDI with standardized Total Water Storage Anomaly (TWSA) from the GRACE satellites for the 2002–2016 period for the Sabarmati and Brahmani River Basins, respectively. (B, D) Comparison of monthly IDI with standardized groundwater table depth anomaly (WTDA) from CGWB for 1996–2016 for the Sabarmati and Brahmani River Basins, respectively.

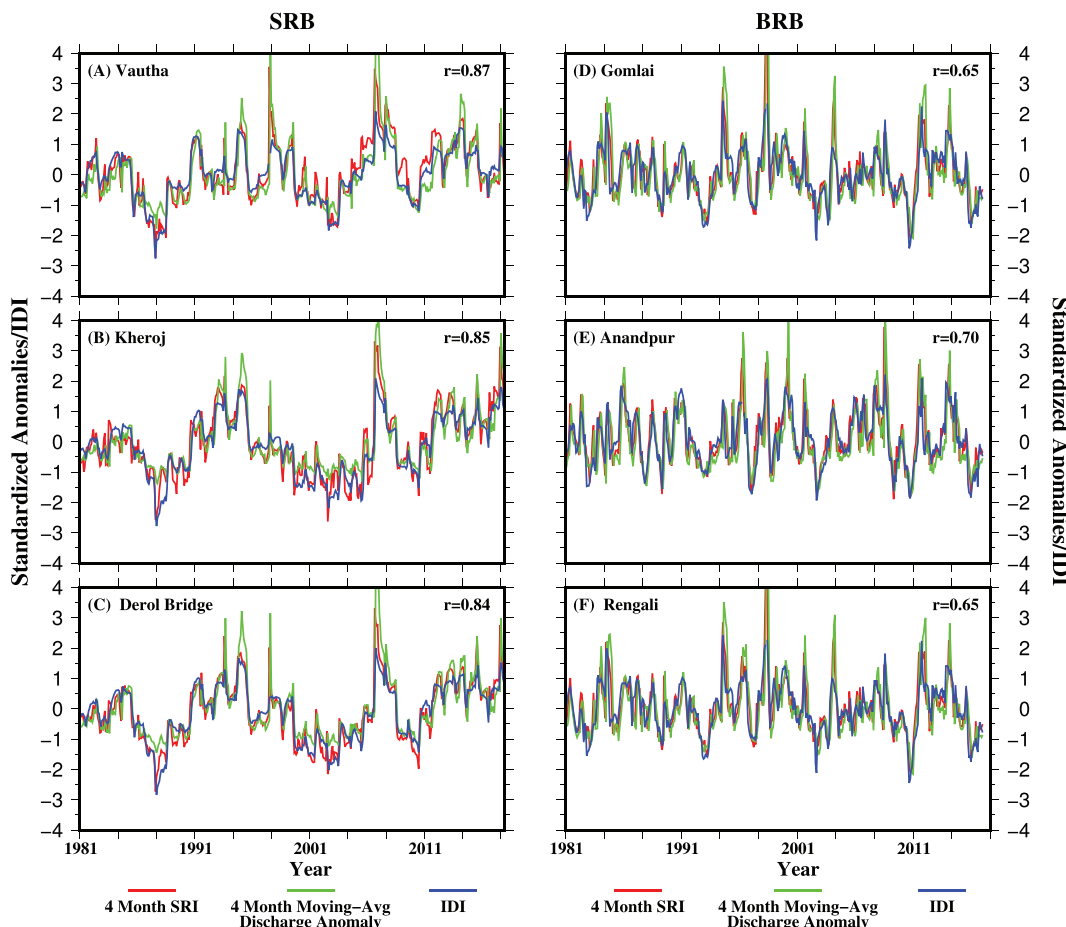


Figure 11. (A–C) Comparison of 1-month IDI with 4-month SRI and 4-month moving averaged VIC-SIMGM simulated discharge anomaly at Vautha, Kheroj, and Derol bridge for the period of 1980–2016, respectively, in the Sabarmati River Basin. (D–F) Same as (A–C) but for Brahmani River Basin.

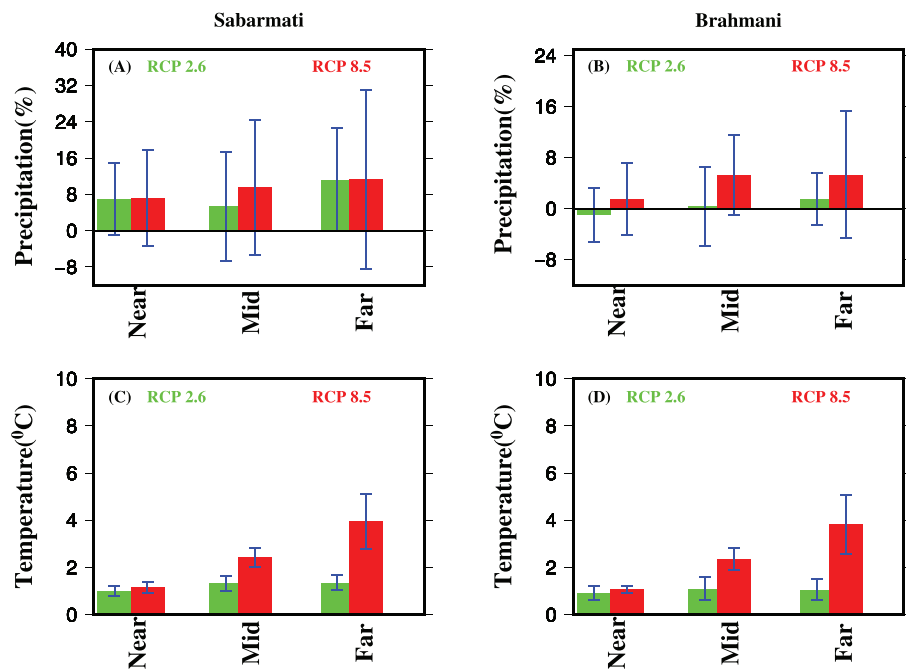


Figure 12. (A, B) The multimodel ensemble mean change in precipitation (%) in the near (2011–2040), mid (2041–2070), and far (2071–2100) periods with reference to the historic period (1971–2000) in Sabarmati and Brahmani River basins, respectively. (C, D) The multimodel ensemble mean change in mean temperature ($^{\circ}\text{C}$) in the near (2011–2040), mid (2041–2070), and far (2071–2100) periods with reference to the historic period (1971–2000) in Sabarmati and Brahmani River basins, respectively.

terminated in September 1990 with the duration of 62 months. The peak intensity of the 1987 drought was significantly higher than the 1965 drought (Table 1). The 2002 drought started in August 1999 and ended in July 2005 and lasted more than 70 months in the Sabarmati River basin. All three major droughts affected the entire basin. The other 11 droughts identified based on IDI were significantly less severe and did not affect the entire SRB (Table 1 and Figure 6).

The most severe droughts in the Brahmani basin occurred in 1966, 1979, and 2010 (Table 2). The longest drought during 1952–2017 with the duration of 71 months started in May 1965 and terminated in April 1971 with average and peak intensities of -0.48 and -1.48 , respectively. The second most severe drought started in May 1979 and terminated in March 1981. The mean and maximum intensities during the 1979–1980 drought period were -0.52 and -1.54 , respectively. The 2010 drought is the most recent severe drought in BRB which started in November 2008 and terminated in June 2011. All three droughts affected more than 95% of the basin area. Apart from this, we identified 13 other droughts that were significantly less severe than these droughts (Table 2 and Figure 7).

Next, we compare drought intensities estimated using IDI, 12-month SPI, 1-month SSI, 1-month SGI, and 4-month SRI to understand the spatial variability of drought in SRB and BRB (Figures 6 and 7). To do so, we selected drought intensities for August 1987, June 2002, and June 2010 where the peak intensity of IDI occurred for the drought spells of 1985–1990, 1999–2005, and 2008–2010 for SRB. Drought based on IDI successfully captures the variability in meteorological, hydrological, and agricultural droughts for all the three (August 1987, June 2002, and June 2010) periods (Figure 6). However, there are expected differences in the areal extent estimated using IDI and the other indices (SSI, SGI, SPI, and SRI), which further highlight the need for IDI that can combine the response of meteorological, hydrological, and agricultural droughts. Similar to SRB, we selected drought intensities for November 1979, August 2002, and August 2010 for the spell of 1979–1981, 2000–2002, and 2008–2011. The drought based on IDI successfully captures the variability related to overall meteorological, agricultural and hydrological droughts in BRB.

Apart from droughts, we also checked if IDI can capture wet spells (with positive IDI values). To do so, we selected three events based on the basin averaged IDI time series in each basin. We find that IDI

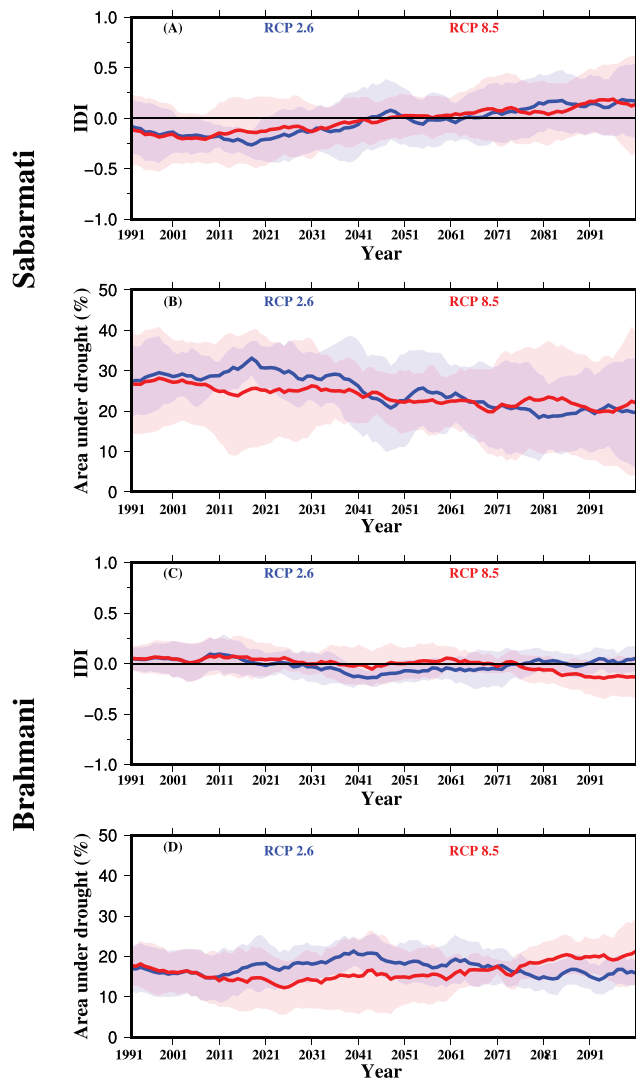


Figure 13. (A, C) Thirty-year moving average IDI for the month of May for Sabarmati and Brahmani River basins for the period of 1961–2100 (1961–1990, 1962–1991, and so on), respectively. (B, D) Thirty-year moving average area under drought (%) for the month of May for Sabarmati and Brahmani River basins for the period of 1961–2100, respectively.

and water table depth anomalies (Figure 10). Moreover, at the three gauge stations, IDI is strongly correlated with streamflow anomalies with a correlation coefficient higher than 0.8 (Figure 11).

Similar to the evaluation of the performance of IDI for the Sabarmati River basin, we tested the spatial and temporal response of IDI in the Brahmani basin using DSI, TWSA, GWSA, groundwater well, and streamflow anomalies during 1952–2017. To do so, we selected August 2002 and August 2010 to compare IDI against the other independent variables that represent hydrological and agricultural droughts (Figure 9). Similar to SRB, we find that IDI captures the vegetation, groundwater, and streamflow droughts successfully during August 2002 and 2010. For instance, we find that almost all of the Brahmani basin was affected by the severe and extreme drought during August 2002 and 2010 that affected agriculture, streamflow, terrestrial, and groundwater storage. We find that IDI is well correlated with TWSA and water table anomalies with a correlation coefficient of about 0.7 (Figure 10). Moreover, IDI can capture the temporal variability in streamflow at the three (Gomlai, Anandpur, and Rengali) stations with a correlation coefficient of more than 0.6

captures spatial variability exhibited by the other indices during the wet events (Figures S6 and S7). Overall, IDI captures both short- and long-term droughts and the integrated responses of meteorological, hydrological, and agricultural droughts in the two basins located in the different climatic and geographical regions.

3.3. Evaluation of IDI

Next, we evaluate IDI against observations of vegetation, terrestrial water storage, groundwater, and streamflow anomalies in both the river basins (Figures 8 and 9). To capture the vegetation drought, we used the monthly Drought Severity Index (DSI: Mu et al., 2013) at 0.05° spatial resolution. In addition to DSI, we used terrestrial and groundwater storage anomalies from the GRACE satellites and in situ observations from CGWB wells to compare with IDI. Moreover, streamflow simulated from the VIC-SIMGM using the observed meteorological forcing as well as observed streamflow (Figure S8) was used to evaluate the performance of IDI. We find that during July 2002, a large part of the Sabarmati river basin was affected by severe drought, especially in the northern and upstream regions of the basin (Figure 8). Our results show that during July 2002, the SRB experienced a severe drought in vegetation conditions as shown by DSI, which is consistent with the response of IDI. Here we note that the scales of IDI and DSI are different. Therefore, DSI exhibits a somewhat lesser intensity than IDI (Figure 8).

Both terrestrial and groundwater storage anomalies estimated using the GRACE data show a widespread drought in July 2002 in SRB, which is well captured in IDI (Figure 8). Since the GRACE data are at a much coarser resolution, drought response in the GRACE is somewhat smoothed than in IDI. Consistent with the GRACE groundwater storage anomalies, in situ data from observational wells located in the Sabarmati River basin also show drought primarily in the northern and central parts of the basin. Moreover, the three streamflow gauge stations show negative streamflow (4-month) anomalies during July 2002. Our results show that IDI can capture the drought variability exhibited by DSI, TWSA, GWSA, groundwater wells, and streamflow anomalies during June 2010. All the independent indicators that capture hydrological and agricultural drought show a response that is consistent with IDI. Also, we also evaluated the temporal dynamics of TWSA, groundwater, and streamflow anomalies (Figures 10, 11, and S8). We find that basin-averaged IDI is well correlated with TWSA

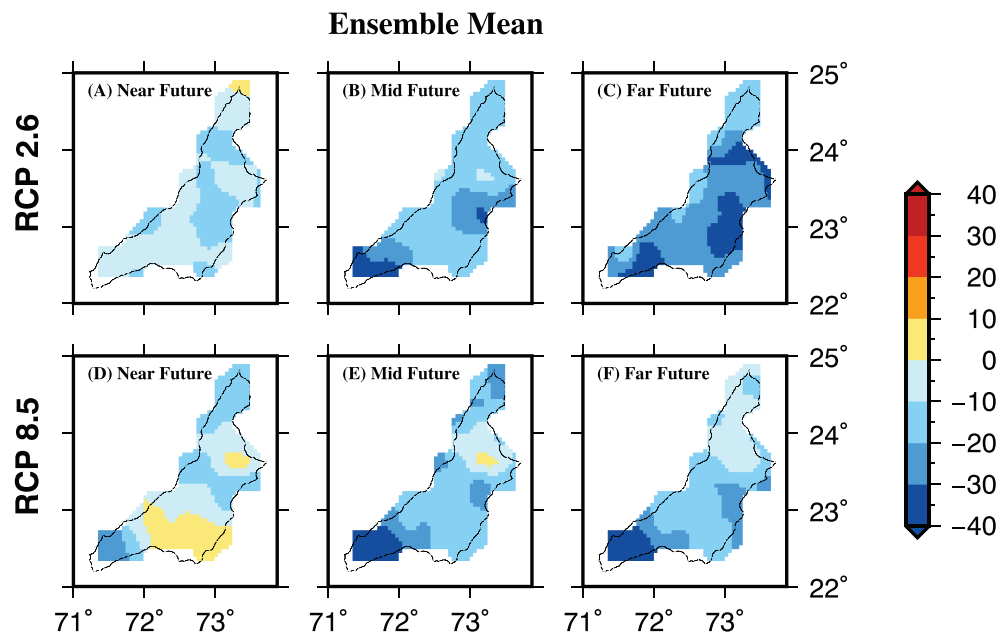


Figure 14. (A, D) Multimodel ensemble mean projected change in the frequency of droughts ($IDI \leq -0.8$) with respect to the historic period (1971–2000) in the near (2011–2040) future under RCP 2.6 and 8.5, respectively. (B, E) Same as (A, D) but for the mid (2041–2070) future, and (C, F) same as (A, D) but for the far (2071–2100) period for the Sabarmati River Basin.

(Figure 11). These results indicate that IDI can effectively capture the response of meteorological, hydrological, and agricultural droughts as well as wet periods (Figures S9 and S10).

3.4. Drought Projections Based on IDI

Finally, we used IDI to develop drought projections for the two (SRB and BRB) river basins using down-scaled and bias-corrected data from the eight (BNU-ESM, CESM1-CAM5, GFDL-ESM 2M, MPI-ESM-LR, NorESM1-M, GFDL-ESM 2G, MIROC-ESM, and MIROC-ESM-CHEM) CMIP5-GCMs. The bias correction was performed using the trend-preserving method (Hempel et al., 2013). We find that bias in precipitation and temperature has significantly improved after the correction (Figures S11–S14).

We estimated ensemble mean projected change in mean annual precipitation (%) and temperature (°C) for the near (2011–2040), mid (2041–2070), and far (2071–2100) periods against the reference of 1971–2000 for both the basins (Figure 12). There is a robust increase in mean annual temperature in both the basins depending on the RCP (2.6 and 8.5; Figure 12). However, the precipitation projections show a large intermodel uncertainty in both the basins. The multimodel ensemble mean precipitation is projected to increase in the Sabarmati basin while both increase and decline are projected for the Brahmani basin (Figure 12). Uncertainty in precipitation projections translates to the projections of IDI at the end of the water year (May) and associated area under drought for the projected future climate in both basins (Figure 13).

We estimated IDI for all the eight GCMs and two RCPs (2.6 and 8.5) for both the basins. Projected changes in the drought frequency (the number of months with $IDI \leq -0.8$) were estimated for the near (2011–2040), mid (2041–2070), and far (2071–2100) periods against the reference of 1971–2000. Our results show a decline in the frequency of droughts in the near, mid, and far periods under both RCP 2.6 and 8.5 in the Sabarmati river basin (Figure 14). The drought frequency is projected to increase in a few regions of the Sabarmati river basin in the near period under the high-emission scenario of RCP 8.5. Therefore, the projected changes in the drought frequency in the Sabarmati river basin can vary with the period (e.g., near, mid, and far) as well as with the emission scenario (RCP 2.6 and 8.5). We find large intermodel variability in the projections of droughts under the warming climate in the Sabarmati river basin (Figures S15 and S16). For instance, out of eight selected GCMs, the four (BNU-ESM, CESM1-CAM5, GFDL-ESM 2G, and MIROC-ESM-CHEM)

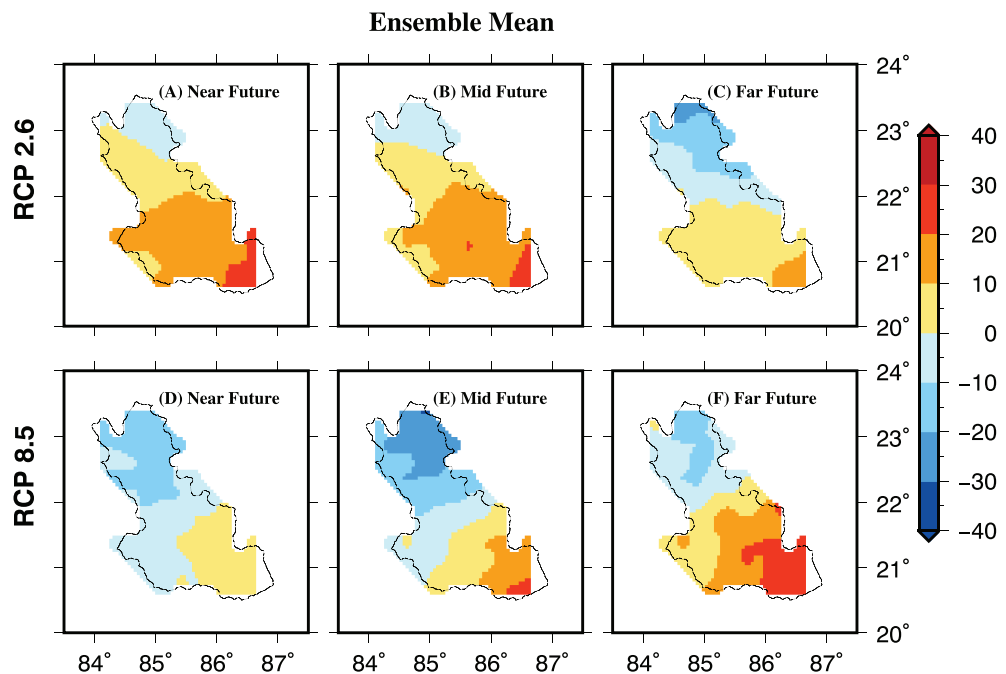


Figure 15. Same as Figure 14 but for the Brahmani River Basin.

show a decline in the frequency of droughts under the warming climate while the other four project an increase. These differences in the projected frequency of droughts in the Sabarmati river basin can be attributed to the changes and associated uncertainty in precipitation and temperature in the GCMs (Figure 12 and Tables S7 and S9).

The drought frequency based on IDI is projected to increase in the Brahmani basin under both RCPs (Figure 15). Moreover, the drought frequency in the Brahmani basin is projected to increase more prominently in the far period under the RCP 8.5. Similar to the Sabarmati river basin, we find a large intermodel variation in the projected changes in the frequency of droughts under the warming climate in the Brahmani basin (Figures S17 and S18). In addition to IDI, we also estimated the drought frequency based on SPI (Figures S19–S22), which shows differences in drought projections in comparison to IDI. The difference in the drought projections based on SPI and IDI further highlights the need for IDI for drought assessment under the warming climate. Overall, our results show that IDI can be used to evaluate the changes in drought characteristics under the warming climate in India. Since IDI is based on the integrated response of meteorological, hydrological, and agricultural droughts and includes the groundwater response, it can provide valuable insights on the water availability and drought under the warming climate in India.

4. Conclusions

Monitoring and assessing the impacts of droughts remain a profound challenge in India primarily because of a large requirement of the number of indicators associated with meteorological, hydrological, and agricultural droughts. Moreover, groundwater storage variability during droughts is often neglected from the drought monitoring and assessment in India. Using 12-month SPI, 4-month SRI, 1-month SSI, and 1-month SGI, we developed IDI that can provide an integrated response of all the three types of droughts and includes groundwater variability. IDI was developed for the period of 1952–2017, which was evaluated against independent observations of DSI, TWSA, GWSA, groundwater well, and streamflow anomalies for the two basins located in the diverse climatic regimes in India. We used IDI to identify the major droughts in the two basins during 1952–2017. Moreover, we used IDI to estimate the changes in the drought frequency in the two basins under the warming climate using the downscaled and bias-corrected projections from the eight CMIP5 models. Based on our findings, the following are the major conclusions:

1. The VIC-SIMGM captured the observed variability in streamflow and groundwater well anomalies in the Sabarmati and Brahmani basins during 1952–2017. The VIC-SIMGM simulated runoff, soil moisture, and groundwater well anomalies were used to construct IDI for the two basins.
2. IDI successfully captures both short- and long-term drought variability of meteorological, hydrological, and agricultural droughts. Drought characteristics identified using IDI showed that there are 14 major droughts that occurred in the Sabarmati River basin. Out of these 14 droughts, the three droughts (1965, 1987, and 2002) were the most severe based on the overall drought severity score. Similarly, out of the 16 droughts identified in the Brahmani basin, the three most severe droughts occurred in 1966, 1979, and 2010.
3. IDI effectively captured the response of vegetation (from DSI), terrestrial and groundwater storage from GRACE, and streamflow and well anomalies for the two basins. Therefore, IDI can be integrated with the current real-time monitoring and forecast systems that are operational in India (https://sites.google.com/a/iitgn.ac.in/high_resolution_south_asia_drought_monitor/).
4. Notwithstanding the high intermodel variability, the multimodel ensemble mean projections based on IDI show a decrease in the drought frequency in the Sabarmati basin. Drought frequency is projected to increase by the mid-21st century under RCP 2.6 in the Brahmani basin.
5. Overall, our findings and analysis show that IDI can be effectively used for drought monitoring and assessment under the current and future climate in India. Moreover, IDI overcomes the shortcoming of the lack of required variability to identify the onset and termination of drought as it integrates the response of several drought indicators and accounts for groundwater storage variability in drought assessments.

Acknowledgments

Data sets used in this study are available from the India Meteorological Department (IMD): www.imd.gov.in; GRACE: <https://grace.jpl.nasa.gov>, and India Water Resources Information System (India-WARIS: <http://www.india-wris.nrsc.gov.in>). The authors acknowledge the financial support from the Ministry of Human Resources Development and National Water Mission of Ministry of Water Resources.

References

- Aadhar, S., & Mishra, V. (2017). High-resolution near real-time drought monitoring in South Asia. *Scientific Data*, 4, 170145. <https://doi.org/10.1038/sdata.2017.145>
- AghaKouchak, A., Farahmand, A., Melton, F. S., Teixeira, J., Anderson, M. C., Wardlow, B. D., & Hain, C. R. (2015). Remote sensing of drought: Progress, challenges and opportunities. *Reviews of Geophysics*, 53, 1–29. <https://doi.org/10.1002/2014RG000456>. Received
- Apurv, T., Sivapalan, M., & Cai, X. (2017). Understanding the role of climate characteristics in drought propagation. *Water Resources Research*, 53, 9304–9329. <https://doi.org/10.1002/2017WR021445>
- Ashfaq, M., Rastogi, D., Mei, R., Touma, D., & Ruby Leung, L. (2017). Sources of errors in the simulation of south Asian summer monsoon in the CMIP5 GCMs. *Climate Dynamics*, 49(1–2), 193–223. <https://doi.org/10.1007/s00382-016-3337-7>
- Asoka, A., Wada, Y., Fishman, R., & Mishra, V. (2018). Strong Linkage Between Precipitation Intensity and Monsoon Season GroundwaterRecharge in India. *Geophysical Research Letters*, 45(11), 5536–5544. <https://doi.org/10.1029/2018GL078466>
- Asoka, A., Gleeson, T., Wada, Y., & Mishra, V. (2017). Relative contribution of monsoon precipitation and pumping to changes in groundwater storage in India. *Nature Geoscience*, 10(2), 109–117. <https://doi.org/10.1038/ngeo2869>
- Beersma, J. J., & Buishand, T. A. (2004). Joint probability of precipitation and discharge deficits in the Netherlands. *Water Resources Research*, 40, W12508. <https://doi.org/10.1029/2004WR003265>
- Castle, S. L., Thomas, B. F., Reager, J. T., Rodell, M., Swenson, S. C., & Famiglietti, J. S. (2014). Groundwater depletion during drought threatens future water security of the Colorado River Basin. *Geophysical Research Letters*, 41, 5904–5911. <https://doi.org/10.1002/2014GL061055>
- Chang, J., Li, Y., Wang, Y., & Yuan, M. (2016). Copula-based drought risk assessment combined with an integrated index in the Wei River Basin, China. *Journal of Hydrology*, 540, 824–834. <https://doi.org/10.1016/j.JHYDROL.2016.06.064>
- Chen, J., Famiglietti, J. S., Scanlon, B. R., & Rodell, M. (2016). *Groundwater storage changes: Present status from GRACE observations*, (pp. 207–227). Cham: Springer. https://doi.org/10.1007/978-3-319-32449-4_9
- Cherkauer, K. A., Bowling, L. C., & Lettenmaier, D. P. (2003). Variable infiltration capacity cold land process model updates. *Global and Planetary Change*, 38(1–2), 151–159. [https://doi.org/10.1016/S0921-8181\(03\)00025-0](https://doi.org/10.1016/S0921-8181(03)00025-0)
- De Michele, C., & Salvadori, G. (2003). A generalized Pareto intensity-duration model of storm rainfall exploiting 2-Copulas. *Journal of Geophysical Research*, 108(D2), 4067. <https://doi.org/10.1029/2002JD002534>
- Dutta, D., Kundu, A., & Patel, N. R. (2013). Predicting agricultural drought in eastern Rajasthan of India using NDVI and standardized precipitation index. *Geocarto International*, 28(3), 192–209. <https://doi.org/10.1080/10106049.2012.679975>
- Favre, A.-C., El Adlouni, S., Perreault, L., Thiémonge, N., & Bobée, B. (2004). Multivariate hydrological frequency analysis using copulas. *Water Resources Research*, 40, W01101. <https://doi.org/10.1029/2003WR002456>
- Gao, H., Tang, Q., Shi, X., Zhu, C., Bohn, T., Su, F., et al. (2009). Chapter 6 Water budget record from Variable Infiltration Capacity (VIC) model. Retrieved from http://eprints.lancs.ac.uk/89407/1/Gao_et_al_VIC_2014.pdf
- Gedney, N., Cox, P. M., Gedney, N., & Cox, P. M. (2003). The sensitivity of global climate model simulations to the representation of soil moisture heterogeneity. *Journal of Hydrometeorology*, 4(6), 1265–1275. [https://doi.org/10.1175/1525-7541\(2003\)004<1265:TSOGCM>2.0.CO;2](https://doi.org/10.1175/1525-7541(2003)004<1265:TSOGCM>2.0.CO;2)
- Genest, C., & Favre, A.-C. (2007). Everything you always wanted to know about Copula modeling but were afraid to ask. *Journal of Hydrologic Engineering*, 12(4), 347–368. [https://doi.org/10.1061/\(ASCE\)1084-0699\(2007\)12:4\(347\)](https://doi.org/10.1061/(ASCE)1084-0699(2007)12:4(347))
- Genest, C., Quesy, J.-F., & Remillard, B. (2006). Goodness-of-fit procedures for Copula models based on the probability integral transformation. *Scandinavian Journal of Statistics*, 33(2), 337–366. <https://doi.org/10.1111/j.1467-9469.2006.00470.x>
- Godfray, H. C. J., Beddington, J. R., Crute, I. R., Haddad, L., Lawrence, D., Muir, J. F., et al. (2010). Food security: The challenge of feeding 9 billion people. *Science (New York, N.Y.)*, 327(5967), 812–818. <https://doi.org/10.1126/science.1185383>

- Grimaldi, S., & Serinaldi, F. (2006). Design hyetograph analysis with 3-copula function. *Hydrological Sciences Journal*, 51(2), 223–238. <https://doi.org/10.1623/hysj.51.2.223>
- Gupta, H. V., Bastidas, L. A., Sorooshian, S., Shuttleworth, W. J., & Yang, Z. L. (1999). Parameter estimation of a land surface scheme using multicriteria methods. *Journal of Geophysical Research*, 104(D16), 19491–19503. <https://doi.org/10.1029/1999JD900154>
- Haddeland, I., Heinke, J., Biemans, H., Eisner, S., Flörke, M., Hanasaki, N., et al. (2014). Global water resources affected by human interventions and climate change. *Proceedings of the National Academy of Sciences of the United States of America*, 111(9), 3251–3256. <https://doi.org/10.1073/pnas.1222475111>
- Hansen, M. C., Defries, R. S., Townshend, J. R. G., & Sohlberg, R. (2000). Global land cover classification at 1 km spatial resolution using a classification tree approach. *International Journal of Remote Sensing*, 21(6–7), 1331–1364. <https://doi.org/10.1080/014311600210209>
- Hao, Z., & AghaKouchak, A. (2013). Multivariate Standardized Drought Index: A parametric multi-index model. *Advances in Water Resources*, 57, 12–18. <https://doi.org/10.1016/J.ADVWATRES.2013.03.009>
- Hao, Z., & Singh, V. (2015). Integrating entropy and copula theories for hydrologic modeling and analysis. *Entropy*, 17(4), 2253–2280. <https://doi.org/10.3390/e17042253>
- Hempel, S., Frieler, K., Warsawski, L., Schewe, J., & Piontek, F. (2013). A trend-preserving bias correction—The ISI-MIP approach. *Earth System Dynamics*, 4(2), 219–236. <https://doi.org/10.5194/esd-4-219-2013>
- Ji, L., & Peters, A. J. (2003). Assessing vegetation response to drought in the northern Great Plains using vegetation and drought indices. *Remote Sensing of Environment*, 87(1), 85–98. [https://doi.org/10.1016/S0034-4257\(03\)00174-3](https://doi.org/10.1016/S0034-4257(03)00174-3)
- Kao, S.-C., & Govindaraju, R. S. (2007). A bivariate frequency analysis of extreme rainfall with implications for design. *Journal of Geophysical Research*, 112, D13119. <https://doi.org/10.1029/2007JD008522>
- Kao, S.-C., & Govindaraju, R. S. (2010). A copula-based joint deficit index for droughts. *Journal of Hydrology*, 380(1–2), 121–134. <https://doi.org/10.1016/J.JHYDROL.2009.10.029>
- Keyantash, J., Dracup, J. A., Keyantash, J., & Dracup, J. A. (2002). The quantification of drought: An evaluation of drought indices. *Bulletin of the American Meteorological Society*, 83(8), 1167–1180. <https://doi.org/10.1175/1520-0477-83.8.1167>
- Koll Roxy, M., Ritika, K., Terray, P., Murtagudde, R., Ashok, K., & Goswami, B. (2015). Drying of Indian subcontinent by rapid Indian Ocean warming and a weakening land-sea thermal gradient. *Nature Communications*, 6. <https://doi.org/10.1038/ncomms8423>
- Kottek, M., Grieser, J., Beck, C., Rudolf, B., & Rubel, F. (2006). World map of the Köppen-Geiger climate classification updated. *Meteorologische Zeitschrift*, 15(3), 259–263. <https://doi.org/10.1127/0941-2948/2006/0130>
- Kuhn, G., Khan, S., Ganguly, A. R., & Branstetter, M. L. (2007). Geospatial-temporal dependence among weekly precipitation extremes with applications to observations and climate model simulations in South America. *Advances in Water Resources*, 30(12), 2401–2423. <https://doi.org/10.1016/J.ADVWATRES.2007.05.006>
- Kumar, R., & Mishra, V. (2019). Decline in surface urban heat island intensity in India during heatwaves. *Environmental Research Communications*, 1(3), 031001. <https://doi.org/10.1088/2515-7620/ab121d>
- Kumar, R., Musuza, J. L., Van Loon, A. F., Teuling, A. J., Barthel, R., Ten Broek, J., et al. (2016). Multiscale evaluation of the Standardized Precipitation Index as a groundwater drought indicator. *Hydrology and Earth System Sciences*, 20(3), 1117–1131. <https://doi.org/10.5194/hess-20-1117-2016>
- Li, B., & Rodell, M. (2015). Evaluation of a model-based groundwater drought indicator in the conterminous U.S. *Journal of Hydrology*, 526, 78–88. <https://doi.org/10.1016/J.JHYDROL.2014.09.027>
- Liang, X., Lettenmaier, D. P., & Wood, E. F. (1996). One-dimensional statistical dynamic representation of subgrid spatial variability of precipitation in the two-layer variable infiltration capacity model. *Journal of Geophysical Research*, 101. <https://doi.org/10.1029/96JD01448>
- Liang, X., Lettenmaier, D. P., Wood, E. F., & Burges, S. J. (1994). A simple hydrologically based model of land surface water and energy fluxes for general circulation models. *Journal of Geophysical Research*, 99(D7), 14415. <https://doi.org/10.1029/94JD00483>
- Liu, W. T., & Kogan, F. N. (1996). Monitoring regional drought using the vegetation condition index. *International Journal of Remote Sensing*, 17(14), 2761–2782. <https://doi.org/10.1080/01431169608949106>
- Liu, Z., Törmärs, T., & Menzel, L. (2016). A probabilistic prediction network for hydrological drought identification and environmental flow assessment. *Water Resources Research*, 52, 6243–6262. <https://doi.org/10.1002/2016WR019106>
- Lloyd-Hughes, B. (2014). The impracticality of a universal drought definition. *Theoretical and Applied Climatology*, 117(3–4), 607–611. <https://doi.org/10.1007/s00704-013-1025-7>
- Lohmann, D., Nolte-holube, R., & Raschke, E. (1996). A large-scale horizontal routing model to be coupled to land surface parametrization schemes. *Tellus A*, 48(5), 708–721. <https://doi.org/10.1034/j.1600-0870.1996.t01-3-00009.x>
- Lohmann, D., Raschke, E., Nijssen, B., & Lettenmaier, D. P. (1998). Regional scale hydrology: II. Application of the VIC-2 L model to the Weser River, Germany. *Hydrological Sciences Journal*, 43(1), 143–158. <https://doi.org/10.1080/0262669809492108>
- Long, D., Chen, X., Scanlon, B. R., Wada, Y., Hong, Y., Singh, V. P., et al. (2016). Have GRACE satellites overestimated groundwater depletion in the Northwest India Aquifer? *Scientific Reports*, 6(1), 24398. <https://doi.org/10.1038/srep24398>
- Ma, M., Ren, L., Singh, V. P., Yang, X., Yuan, F., & Jiang, S. (2014). New variants of the Palmer drought scheme capable of integrated utility. *Journal of Hydrology*, 519, 1108–1119. <https://doi.org/10.1016/J.JHYDROL.2014.08.041>
- Maurer, E. P., Wood, A. W., Adam, J. C., Lettenmaier, D. P., & Nijssen, B. (2002). A long-term hydrologically based dataset of land surface fluxes and states for the conterminous United States*. *Journal of Climate*, 15(22), 3237–3251. [https://doi.org/10.1175/1520-0442\(2002\)015<3237:ALTHBD>2.0.CO;2](https://doi.org/10.1175/1520-0442(2002)015<3237:ALTHBD>2.0.CO;2)
- McKee, T. B., Doesken, N. J., & Kleist, J. (1993). The relationship of drought frequency and duration to time scales. Eighth Conference on Applied Climatology. Retrieved from <https://climate.colostate.edu/pdfs/relationshipofdroughtfrequency.pdf>
- McSweeney, C. F., & Jones, R. G. (2016). How representative is the spread of climate projections from the 5 CMIP5 GCMs used in ISI-MIP? *Climatic Services*, 1, 24–29. <https://doi.org/10.1016/J.CLISER.2016.02.001>
- Mishra, A. K., & Singh, V. P. (2010). A review of drought concepts. *Journal of Hydrology*, 391(1–2), 202–216. <https://doi.org/10.1016/J.JHYDROL.2010.07.012>
- Mishra, V., Aadhar, S., Asoka, A., Pai, S., & Kumar, R. (2016). On the frequency of the 2015 monsoon season drought in the Indo-Gangetic Plain. *Geophysical Research Letters*, 43, 12,102–12,112. <https://doi.org/10.1002/2016GL071407>
- Mishra, V., Cherkauer, K. A., Bowling, L. C., Mishra, V., Cherkauer, K. A., & Bowling, L. C. (2010). Parameterization of lakes and wetlands for energy and water balance studies in the Great Lakes Region*. *Journal of Hydrometeorology*, 11(5), 1057–1082. <https://doi.org/10.1175/2010JHM1207.1>
- Mishra, V., Shah, R., Azhar, S., Shah, H., Modi, P., & Kumar, R. (2018). Reconstruction of droughts in India using multiple land-surface models (1951–2015). *Hydrology and Earth System Sciences*, 22(4), 2269–2284. <https://doi.org/10.5194/hess-22-2269-2018>

- Mishra, V., Shah, R., Thrasher, B., Mishra, V., Shah, R., & Thrasher, B. (2014). Soil moisture droughts under the retrospective and projected climate in India*. *Journal of Hydrometeorology*, 15(6), 2267–2292. <https://doi.org/10.1175/JHM-D-13-0177.1>
- Mishra, V., Smoliak, B. V., Lettenmaier, D. P., & Wallace, J. M. (2012). A prominent pattern of year-to-year variability in Indian Summer Monsoon Rainfall. *PNAS*, 109(19), 7213–7217. <https://doi.org/10.1073/pnas.1119150109>
- Mishra, V., Tiwari, A. D., Aadhar, S., Shah, R., Xiao, M., Pai, D. S., & Lettenmaier, D. (2019). Drought and famine in India, 1870–2016. *Geophysical Research Letters*, 46, 2075–2083. <https://doi.org/10.1029/2018GL081477>
- Mo, K. C. (2011). Drought onset and recovery over the United States. *Journal of Geophysical Research*, 116, D20106. <https://doi.org/10.1029/2011JD016168>
- Moss, R. H., Edmonds, J. A., Hibbard, K. A., Manning, M. R., Rose, S. K., van Vuuren, D. P., et al. (2010). The next generation of scenarios for climate change research and assessment. *Nature*, 463(7282), 747–756. <https://doi.org/10.1038/nature08823>
- Mu, Q., Zhao, M., Kimball, J. S., McDowell, N. G., & Running, S. W. (2013). A remotely sensed global terrestrial drought severity index. *Bulletin of the American Meteorological Society*, 94(1), 83–98. <https://doi.org/10.1175/BAMS-D-11-00213.1>
- Nash, J. E., & Sutcliffe, J. V. (1970). River flow forecasting through conceptual models part I — A discussion of principles. *Journal of Hydrology*, 10(3), 282–290. [https://doi.org/10.1016/0022-1694\(70\)90255-6](https://doi.org/10.1016/0022-1694(70)90255-6)
- Niu, G.-Y., Yang, Z.-L., Dickinson, R. E., Gulden, L. E., & Su, H. (2007). Development of a simple groundwater model for use in climate models and evaluation with gravity recovery and climate experiment data. *Journal of Geophysical Research*, 112, D07103. <https://doi.org/10.1029/2006JD007522>
- Palmer, W. C. (1965). Meteorological drought, Research paper no. 45. US Weather Bureau, Washington, DC, 58.
- Pai, D. S., Sridhar, L., Badwaik, M. R., & Rajeevan, M. (2015). Analysis of the daily rainfall events over India using a new long period (1901–2010) high resolution ($0.25^\circ \times 0.25^\circ$) gridded rainfall data set. *Climate Dynamics*, 45(3–4), 755–776. <https://doi.org/10.1007/s00382-014-2307-1>
- Rana, S., McGregor, J., Renwick, J., Rana, S., McGregor, J., & Renwick, J. (2015). Precipitation seasonality over the Indian subcontinent: An evaluation of gauge, reanalyses, and satellite retrievals. *Journal of Hydrometeorology*, 16(2), 631–651. <https://doi.org/10.1175/JHM-D-14-0106.1>
- Renard, B., & Lang, M. (2007). Use of a Gaussian copula for multivariate extreme value analysis: Some case studies in hydrology. *Advances in Water Resources*, 30(4), 897–912 Retrieved from. <https://www.sciencedirect.com/science/article/pii/S0309170806001461>
- Rodell, B. M., Houser, P. R., Jambor, U., Gottschalck, J., Mitchell, K., Meng, C. J., et al. (2004). The global land data assimilation system This powerful new land surface modeling system integrates data from advanced observing systems to support improved forecast model initialization and hydrometeorological investigations. <https://doi.org/10.1175/BAMS-85-3-381>
- Rodell, M., Velicogna, I., & Famiglietti, J. S. (2009). Satellite-based estimates of groundwater depletion in India. *Nature*, 460(7258), 999–1002. <https://doi.org/10.1038/nature08238>
- Rosenberg, E. A., Clark, E. A., Steinemann, A. C., & Lettenmaier, D. P. (2013). On the contribution of groundwater storage to interannual streamflow anomalies in the Colorado River basin. *Hydrology and Earth System Sciences*, 17(4), 1475–1491. <https://doi.org/10.5194/hess-17-1475-2013>
- Saghafian, B., & Mehdikhani, H. (2014). Drought characterization using a new copula-based trivariate approach. *Natural Hazards*, 72(3), 1391–1407. <https://doi.org/10.1007/s11069-013-0921-6>
- Schewe, J., Heinke, J., Gerten, D., Haddeland, I., Arnell, N. W., Clark, D. B., et al. (2014). Multimodel assessment of water scarcity under climate change. *Proceedings of the National Academy of Sciences of the United States of America*, 111(9), 3245–3250. <https://doi.org/10.1073/pnas.1222460110>
- Shah, H. L., Mishra, V., Shah, H. L., & Mishra, V. (2016a). Hydrologic changes in Indian subcontinental river basins (1901–2012). *Journal of Hydrometeorology*, 17(10), 2667–2687. <https://doi.org/10.1175/JHM-D-15-0231.1>
- Shah, H. L., Mishra, V., Shah, H. L., & Mishra, V. (2016b). Uncertainty and bias in satellite-based precipitation estimates over Indian subcontinental basins: implications for real-time streamflow simulation and flood prediction*. *Journal of Hydrometeorology*, 17(2), 615–636. <https://doi.org/10.1175/JHM-D-15-0115.1>
- Shah, H. L., Zhou, T., Huang, M., & Mishra, V. (2019). Strong influence of irrigation on water budget and land surface temperature in Indian subcontinental river basins. *Journal of Geophysical Research: Atmospheres*, 124, 1449–1462. <https://doi.org/10.1029/2018JD029132>
- Shah, R. D., & Mishra, V. (2015). Development of an Experimental Near-Real-Time Drought Monitor for India*. *Journal of Hydrometeorology*, 16(1), 327–345. <https://doi.org/10.1175/JHM-D-14-0041.1>
- Sheffield, J., Goteti, G., Wen, F., & Wood, E. F. (2004). A simulated soil moisture based drought analysis for the United States. *Journal of Geophysical Research*, 109, D24108. <https://doi.org/10.1029/2004JD005182>
- Sheffield, J., & Wood, E. F. (2007). Characteristics of global and regional drought, 1950–2000: Analysis of soil moisture data from off-line simulation of the terrestrial hydrologic cycle. *Journal of Geophysical Research*, 112, D17115. <https://doi.org/10.1029/2006JD008288>
- Shepard, D. S. (1984). Computer mapping: The SYMAP interpolation algorithm. In *Spatial Statistics and Models*, (pp. 133–145). Dordrecht: Springer Netherlands. https://doi.org/10.1007/978-94-017-3048-8_7
- Shiau, J., Wang, H., & Tsai, C.-T. (2006). Bivariate frequency analysis of floods using copulas1. *Journal of the American Water Resources Association*, 42(6), 1549–1564 Retrieved from <https://onlinelibrary.wiley.com/doi/abs/10.1111/j.1752-1688.2006.tb06020.x>
- Shiau, J. T. (2006). Fitting drought duration and severity with two-dimensional copulas. *Water Resources Management*, 20(5), 795–815. <https://doi.org/10.1007/s11269-005-9008-9>
- Shukla, S., Steinemann, A. C., & Lettenmaier, D. P. (2011). Drought Monitoring for Washington State: Indicators and Applications. *Journal of Hydrometeorology*, 12(1), 66–83. <https://doi.org/10.1175/2010JHM1307.1>
- Shukla, S., & Wood, A. W. (2008). Use of a standardized runoff index for characterizing hydrologic drought. *Geophysical Research Letters*, 35, L02405. <https://doi.org/10.1029/2007GL032487>
- Sinha, D., Syed, T. H., Famiglietti, J. S., Reager, J. T., & Thomas, R. C. (2017). Characterizing drought in India using GRACE observations of terrestrial water storage deficit. *Journal of Hydrometeorology*, 18(2), 381–396. <https://doi.org/10.1175/JHM-D-16-0047.1>
- Sklar, M. (1959). Fonctions de répartition à n dimensions et leurs marges. *Publications de l'Institut de statistique de l'Université de Paris*, 8, 229–231. Retrieved from. <https://ci.nii.ac.jp/naid/10011938360/>
- Song, S., & Singh, V. P. (2010). Meta-elliptical copulas for drought frequency analysis of periodic hydrologic data. *Stochastic Environmental Research and Risk Assessment*, 24(3), 425–444. <https://doi.org/10.1007/s00477-009-0331-1>
- Srivastava, A. K., Rajeevan, M., & Kshirsagar, S. R. (2009). Development of a high resolution daily gridded temperature data set (1969–2005) for the Indian region. *Atmospheric Science Letters*, 10(4). <https://doi.org/10.1002/asl.232>
- Svoboda, M., LeComte, D., Hayes, M., Heim, R., Gleason, K., Angel, J., et al. (2002). The drought monitor. *Bulletin of the American Meteorological Society*, 83(8), 1181–1190. <https://doi.org/10.1175/1520-0477-83.8.1181>

- Switzerland, G.. (1999). Note World Meteorological Organization. Retrieved from https://library.wmo.int/doc_num.php?explnum_id=3459
- Taylor, K. E., Stouffer, R. J., Meehl, G. A., Taylor, K. E., Stouffer, R. J., & Meehl, G. A. (2012). An Overview of CMIP5 and the experiment design. *Bulletin of the American Meteorological Society*, 93(4), 485–498. <https://doi.org/10.1175/BAMS-D-11-00094.1>
- Thomas, B. F., & Famiglietti, J. S. (2019). Identifying climate-induced groundwater depletion in GRACE observations. *Scientific Reports*, 9(1), 4124. <https://doi.org/10.1038/s41598-019-40155-y>
- Thomas, B. F., Famiglietti, J. S., Landerer, F. W., Wiese, D. N., Molotch, N. P., & Argus, D. F. (2017). GRACE groundwater drought index: Evaluation of California Central Valley groundwater drought. *Remote Sensing of Environment*, 198, 384–392. <https://doi.org/10.1016/J.RSE.2017.06.026>
- Tiwari, V. M., Wahr, J., & Swenson, S. (2009). Dwindling groundwater resources in northern India, from satellite gravity observations. *Geophysical Research Letters*, 36, L18401. <https://doi.org/10.1029/2009GL039401>
- Van Loon, A., Kumar, R., Mishra, V. (2017). Testing the use of standardised indices and GRACE satellite data to estimate the European 2015 groundwater drought in near-real time. *Researchgate.Net*. Retrieved from
- Van Loon, A. F. (2015). Hydrological drought explained. *Wiley Interdisciplinary Reviews Water*, 2(4), 359–392. <https://doi.org/10.1002/wat2.1085>
- van Vliet, M. T. H., Wiberg, D., Leduc, S., & Riahi, K. (2016). Power-generation system vulnerability and adaptation to changes in climate and water resources. *Nature Climate Change*, 6(4), 375–380. <https://doi.org/10.1038/nclimate2903>
- Vicente-Serrano, S. M., Beguería, S., López-Moreno, J. I., Vicente-Serrano, S. M., Beguería, S., & López-Moreno, J. I. (2010). A multiscalar drought index sensitive to global warming: The standardized precipitation evapotranspiration index. *Journal of Climate*, 23(7), 1696–1718. <https://doi.org/10.1175/2009JCLI2909.1>
- Wan, Z., Wang, P., & Li, X. (2004). Using MODIS land surface temperature and normalized difference vegetation index products for monitoring drought in the southern Great Plains, USA. *International Journal of Remote Sensing*, 25(1), 61–72. <https://doi.org/10.1080/0143116031000115328>
- Wang, C., Chang, N.-B., & Yeh, G.-T. (2009). Copula-based flood frequency (COFF) analysis at the confluences of river systems. *Hydrological Processes*, 23(10), 1471–1486. <https://doi.org/10.1002/hyp.7273>
- Wang, L., & Qu, J. J. (2009). Satellite remote sensing applications for surface soil moisture monitoring: A review. *Frontiers of Earth Science in China*, 3(2), 237–247. <https://doi.org/10.1007/s11707-009-0023-7>
- Wilhite, D. A. (2005). In D. A. Wilhite (Ed.), *Drought and water crises*. Boca Raton: CRC Press. <https://doi.org/10.1201/9781420028386>
- Wilhite, D. A., & Glantz, M. H. (1985). Understanding: The drought phenomenon: The role of definitions. *Water International*, 10(3), 111–120. <https://doi.org/10.1080/02508068508686328>
- Yeh, P. J.-F., Eltahir, E. A. B., Yeh, P. J.-F., & Eltahir, E. A. B. (2005). Representation of water table dynamics in a land surface scheme. Part I: Model development. *Journal of Climate*, 18(12), 1861–1880. <https://doi.org/10.1175/JCLI3330.1>
- Zargar, A., Sadiq, R., Naser, B., & Khan, F. I. (2011). A review of drought indices. *Environmental Reviews*, 19(NA), 333–349. <https://doi.org/10.1139/a11-013>
- Zhang, L., & Singh, V. P. (2006). Bivariate flood frequency analysis using the copula method. *Journal of Hydrologic Engineering*, 11(2), 150–164. [https://doi.org/10.1061/\(ASCE\)1084-0699\(2006\)11:2\(150\)](https://doi.org/10.1061/(ASCE)1084-0699(2006)11:2(150))
- Zhang, L., & Singh, V. P. (2007). Bivariate rainfall frequency distributions using Archimedean copulas. *Journal of Hydrology*, 332(1–2), 93–109. <https://doi.org/10.1016/J.JHYDROL.2006.06.033>